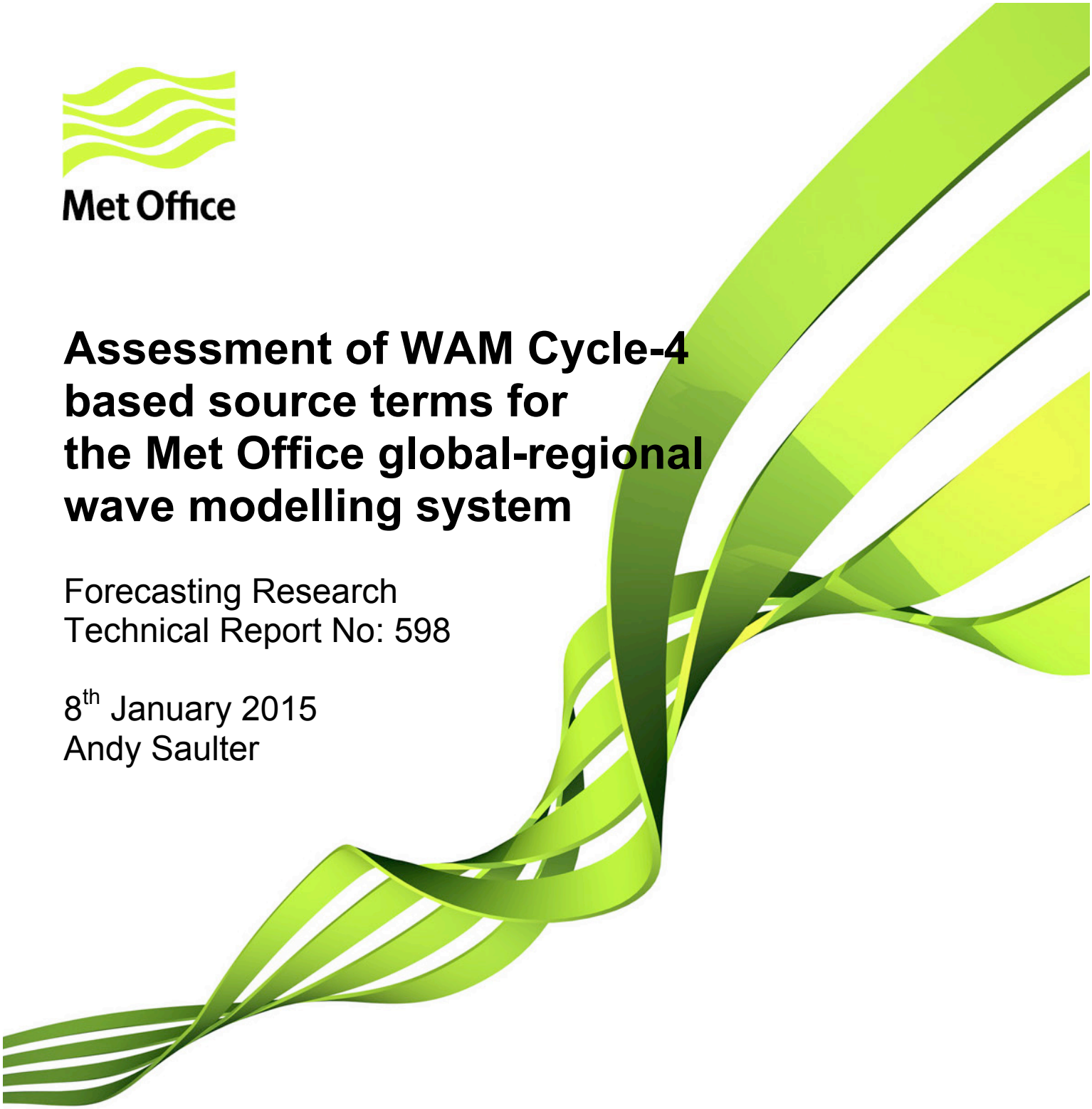

Assessment of WAM Cycle-4 based source terms for the Met Office global-regional wave modelling system

Forecasting Research
Technical Report No: 598

8th January 2015

Andy Saulter

Contents

Executive Summary **3**

1. The Met Office operational wave model suite **4**

2. Source term choices in WAVEWATCH III vn3.14 ..... **6**

3. Idealised wave growth and dissipation tests **9**

4. Global wave model assessment **19**

4.1 Global comparison with satellite altimetry 19

4.2 Regional comparison with in-situ observations 29

4.3 In-situ observation verification in 'boundary condition' regions 42

5. Test3M impacts on regional wave models **48**

6. Spatial impacts of transition from TCOP to TS3M **52**

7. Conclusions and discussion **57**

7.1. Discussion 57

8. References **60**

© Crown copyright 2011

© Crown copyright 2011

Executive Summary

This report describes results of acceptance tests for a revised source term physics scheme applied to the Met Office global wave model. The model is used at the Met Office for global ocean surface wave forecasting and also as a boundary condition for a number of (one-way) nested regional systems. The operational configurations described in this report use WAVEWATCH III (WWIII) vn3.14 as their code-base.

Candidate pschemes tested were based on WWIII vn3.14 flavours of the Tolman and Chalikov (1996), WAM Cycle-4 (Komen et al., 1994) and Ardhuin et al. (2010) source term parameterisations. In addition the tests assessed the performance of a hybrid WAM-Swell scheme, in which the WAM growth and dissipation terms were used in tandem with the swell dissipation parameterisation from the Ardhuin et al. (2010) scheme.

All the schemes were shown to have strengths and weaknesses, in terms of their verification against remote sensed and in-situ observations. However, the study was able to identify the hybrid WAM-Swell scheme (TS3M) as a successor package to the Tolman and Chalikov (1996) source terms for use in the operational global model.

Compared to the present operational scheme, verification has suggested that TS3M will lead to an approximate 5% improvement in significant wave height RMSE and a 10% improvement in mean zero-upcrossing period RMSE. The majority of these improvements will be expected to be obtained in mid-high latitude storm tracks, and are associated with a better representation of wind-sea for storms generating waves over short to moderate fetches. These improvements are offset by a negative significant wave height and positive peak period bias in swell dominated regions of the global ocean.

Impacts of the global model physics change on wave boundary conditions were tested for UK and European regional wave models run at the Met Office. The impact of the change was shown to be limited and neutral overall. Adopting TS3M in the regional models did not lead to any improvements over the WAM Cycle-4 scheme presently used in these models.

It is anticipated that the TS3M scheme will be introduced to the Met Office operational global wave model in early 2015, following Parallel Suite 35.

© Crown copyright 2011

1. The Met Office operational wave model suite

Operational wave models run at the Met Office are presently based on WAVEWATCH III version 3.14 (WWIII, Tolman, 2009). Key operational configurations used for Global, European and UK wave forecasting are shown in Figure 1.1.

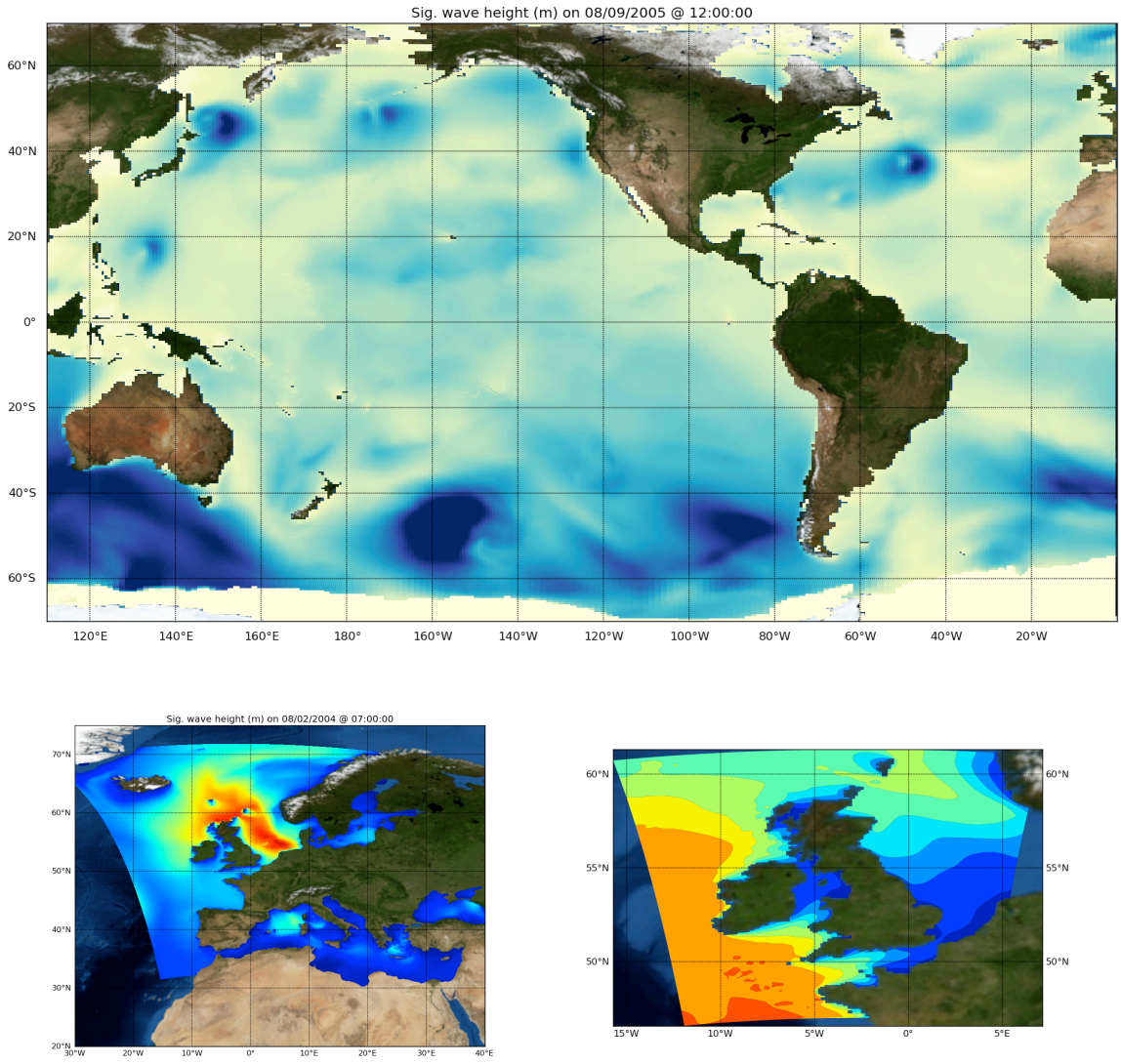

Figure 1.1. Met Office wave model domains: (top) 35km central grid for the Global wave model, (bottom left) 8km the European model (rotated grid) and (bottom right) 4km UK model (rotated grid). The European and UK domains both take boundary conditions from the Global wave model.

© Crown copyright 2011

The global configuration uses a ‘strip grid’ comprising two-way nested 0.3° latitude by 0.8° longitude northern and southern high latitude grids, which are connected to a 0.3° latitude by 0.4° longitude central domain. The present source term scheme for this model is based on parameterisations described by Tolman and Chalikov (1996).

European and UK regional wave models (Figure 1.1) are both constructed on rotated pole grids, in order to limit north-south differentials in longitudinal cell size. The European model is resolved at approximately 8km and the UK model at approximately 4km. Since January 2013 the two models have used a WAM Cycle-4 based source term scheme (Komen et al., 1994), following the tuning described by Bidlot (2012, denoted hereafter as EC12). The choice to move to a WAM based scheme (from the Tolman and Chalikov scheme) was motivated by a need to improve the forecast of rapidly developing waves under storm winds in fetch / duration limited conditions common to UK shelf seas.

© Crown copyright 2011

2. Source term choices in WAVEWATCH III vn3.14

Using two distinct parameterisations in global and regional models leads to the possibility of inconsistencies in the wave spectra passed across model boundaries. In principle such inconsistencies may subsequently impact wave development in the regional models. Recent improvements in verification scores from Meteo France and NCEP global wave models have been attributed to the adoption of flavours of the European Centre WAM (Bidlot, 2012) and Ardhuin et al. (2010, hereafter ARDV) based source term schemes respectively. Both were motivating factors for the Met Office to re-evaluate its choice of global model source terms.

In this study four candidate schemes, as coded in WWIII vn3.14, were compared:

1. The Met Office operational flavour of the Tolman and Chalikov (1996) scheme, denoted hereafter as TCOP.

2. The EC12 WAM Cycle-4 scheme.

3. An ARDV scheme.

4. A hybrid WAM-Swell scheme, in which the WAM parameterisations for growth and dissipation were applied in conjunction with the Ardhuin et al. (2010) parameterisation for dissipation of long period swell.

The settings for each scheme are provided in Table 1. All tests used the standard discrete interaction approximation (DIA) scheme of Hasselmann et al. (1987) to parameterise nonlinear four wave interactions, based on the settings described in Tolman (2009, Section 2.3, Table 2.1). For all runs the spectral resolution of the models was set at 30 frequencies (factor 1.1 logarithmic progression from 0.04118Hz) and 24 directions.

As documented by other authors (e.g. Ardhuin et al., 2010) and discussed in Section 3 of this report, the Tolman and Chalikov (1996) physics function rather differently to any WAM based source terms. From the perspective of this study, the key differentiators between the EC12 and ARDV approaches are in terms of wave dissipation, since both models use the growth term described by Janssen (1991). EC12 uses dissipation following Janssen (1994) and further modified by Bidlot et al. (2007), whilst the ARDV scheme in WWIII vn3.14 is based on a semi-empirical dissipation function, following field

© Crown copyright 2011

experiments by Banner et al. (2000) and Babanin et al. (2001). ARDV also includes an explicit swell dissipation function following observations by Collard et al. (2009). No swell dissipation is included in the default WAM parameterisation coded in WWIII vn3.14.

The hybrid WAM-Swell scheme attempts to address this deficiency by using WAM dissipation and ARDV swell dissipation in combination. It was recognised that this scheme may 'double count' dissipation of long period energy. As a result, a large number of runs were made in order to tune the hybrid scheme, with the settings described in this document (hereafter denoted TS3M) found to be amongst the best performing. The fact that the parameter settings for TS3M (Table 1) do not depart significantly from the other source term schemes was encouraging when considering TS3M as a valid candidate scheme for testing.

© Crown copyright 2011

Table 1. Source term parameter settings for test schemes (where different from WWIII nv3.14 defaults, see Tolman, 2009, Section 2).

Test name	WWIII vn3.14 source term switch	Input source term (SIN) settings	Dissipation source term (SDS) settings
TCOP	ST2	STABSH = 1.40 SWELLF = 0.12	
EC12	ST3	ZALP = 0.008 ALPHA0 = 0.006	SDSC1 = -1.33 SDSDELTA1 = 0.5 SDSDELTA2 = 0.5
ARDV	ST3	BETAMAX = 1.75 ZALP = 0.007 TAUWSHELTER = 0 SWELLFPAR = 3 SWELLF = 0.5 SWELLF2 = -0.018 SWELLF3 = 0.015 SWELLF4 = 100000 SWELLF5 = 0.8 Z0RAT = 0.04 Z0MAX = 0.002	SDSC1 = 0.0 WMEANP = 0.5 WMEANPTAIL = 0.5 SDSDELTA1 = 0.0 SDSDELTA2 = 0.0 SDSC2 = -0.000012 SDSLF = 0.0 SDSHF = 0.0 SDSBR = 0.00085 SDSBR2 = 0.8 SDSC4 = 1.0 SDSP = 2.0 SDS6 = 0.3
TS3M	ST3	BETAMAX = 1.16 ZALP = 0.01 ALPHA0 = 0.006 SWELLFPAR = 3 SWELLF = 0.5 SWELLF2 = -0.009 SWELLF3 = -0.015 SWELLF4 = 100000 SWELLF5 = 0.9 Z0RAT = 0.04	SDSC1 = -1.33 SDSDELTA1 = 0.5 SDSDELTA2 = 0.5

© Crown copyright 2011

3. Idealised wave growth and dissipation tests

A single point model was used to assess differentials in behaviour of the test schemes in two different scenarios. In the first series of tests, wave energy was developed ('grown') from a calm state, for various constant wind settings. The second set of tests assessed dissipation from a well developed sea condition under weak winds (to simulate swell propagation through the tropics).

Figures 3.1-3.4 provide an illustrative example of the different behaviours of each source term under moderately strong wind forcing conditions (of $10ms^{-1}$) in deep water. In these figures an additional scheme in common use by WAM models, following Bidlot et al. (2005, denoted BJA), is also shown. This scheme is the default flavour of WAM in WWIII vn3.14. In each figure the top panel shows the (one-dimensional) frequency spectrum developed by the model. The significant wave height (Hs) values in the panel caption correspond to the values achieved by each scheme, following the order in the figure legend. The second panel from top shows the contribution from the 'input' source term, including 'negative inputs' for schemes that consider swell dissipation as an effect of wave momentum transfer to the atmosphere (TCOP, ARDV, TS3M). The third panel from top is the contribution from the dissipation term. The fourth panel describes the contribution from the nonlinear interaction (DIA) term. Although the settings for this term were the same for all schemes, the DIA reacts to the shape of the wave spectrum and will therefore vary for each of the spectra developed using the different schemes. The bottom panel shows the overall 'source term balance' that is applied to the wave spectrum at the model integration step.

In the early growth stage (after 6 hours, Figure 3.1), development of the WAM based schemes (BJA, EC12, TS3M) follow a similar pattern. Input energy, for these schemes and ARDV, is predominantly around a peak frequency of approximately 0.2Hz. ARDV also has strong inputs at higher frequencies. Dissipation in ARDV is significantly higher than for the other source terms. TCOP behaves significantly differently, developing weaker waves at a peak frequency close to 0.25Hz. Compared to the other source terms, TCOP has relatively weak input and dissipation. In all cases, the balance of the source terms are such that the profile of spectral change closely follows the shape of the nonlinear term.

12 hours into the growth cycle (Figure 3.2), the development of waves under the EC12 scheme has slowed relative to BJA and TS3M. These differences are related to the

© Crown copyright 2011

setting for ZALP (see Ardhuin et al., 2010 also). Hs and spectral distribution of energy are similar in ARDV and EC12, although the input and dissipation terms remain different. Hs in the TCOP scheme is similar to the other models, but at a higher frequency – the TCOP scheme is 'catching up' due to a higher differential between input and dissipation terms than the other schemes.

After 24 and 48 hours of growth (Figures 3.3 and 3.4 respectively) the highest Hs values are generated by TCOP. After 48 hours peak periods from TCOP are consistent with the other schemes. The rate of change in the wave spectrum for all schemes become reduced at this stage of growth as the sea-state tends toward a fully developed condition. ARDV continues to show a different input-dissipation behaviour at high frequencies (greater than 0.3Hz) compared to the other schemes. The source term balance for all terms is broadly similar at 24 hours (Figure 3.3), whilst ARDV and TCOP are still actively affecting the spectrum at 48 hours (Figure 3.4). The Hs values generated by the different schemes after 48 hours range from 2.11m (EC12) to 2.65m (TCOP). In comparison, manual methods (following the nomogram of Breugem and Holthuijsen, 2006) predict a wave height just over 2.5m.

Figures 3.6-3.8 illustrate behaviour in weakly dissipative conditions representing swell propagation away from a generating storm. A caveat for these experiments is that, within the single point model, dispersion effects associated with swell propagation are not accounted for. For each scheme an energetic sea was developed by forcing the model for 24 hours using 15ms^{-1} winds (Figure 3.5). The spectrum that developed was then 'released' into a light wind situation (4ms^{-1}), with the wind set both with the wave direction (e.g. Figures 3.6-3.7) and against the wave direction (e.g, Figure 3.8).

In Figures 3.6-3.8 the input terms for BJA and EC12 tend toward zero, i.e. momentum transfer from atmosphere to ocean, or vice versa, is considered negligible. ARDV, TS3M and TCOP input terms are negative around the peak of the wave spectrum (representing swell dissipation) and of a similar order to the BJA and EC12 dissipation term. TCOP dissipation is negligible, whilst ARDV and TS3M dissipation scale similarly to BJA and EC12. In all cases the negative input-dissipation contribution to the source term balance is only approximately 25-50% of the contribution from the nonlinear term. Thus the nonlinear term has a key influence on spectral change. The overall drop in Hs for following wind conditions after 36 hours ranges from 1.25m (EC12) to 1.64m (TS3M). For headwind conditions Hs is diminished by between 1.25m (EC12, note this term and BJA are insensitive to wind direction) and 1.74m (TS3M).

© Crown copyright 2011

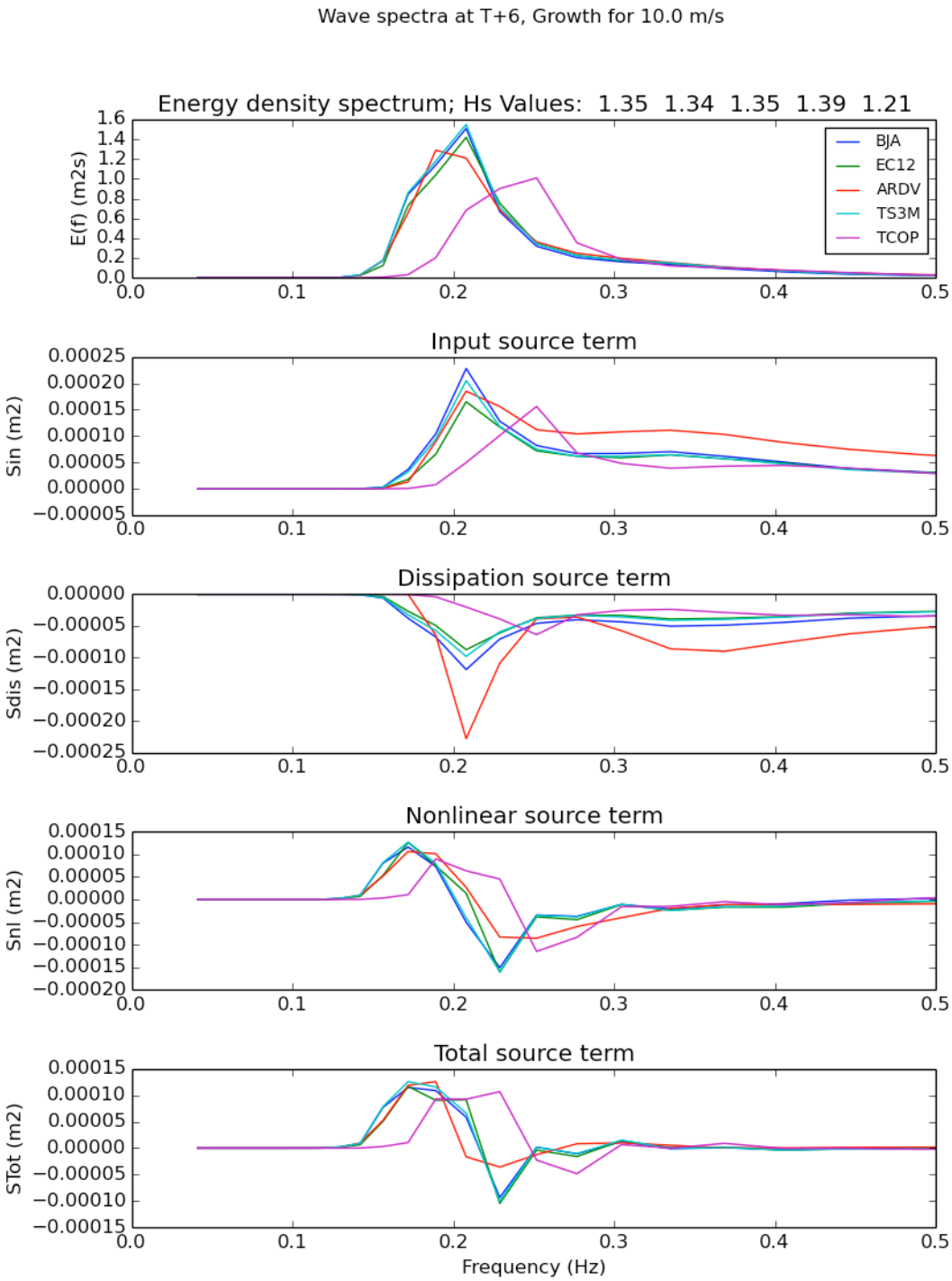

Figure 3.1. Wave spectra and source terms from growth test with constant wind speed at 10ms^{-1}. Model state after 6 hours forcing from calm.

© Crown copyright 2011

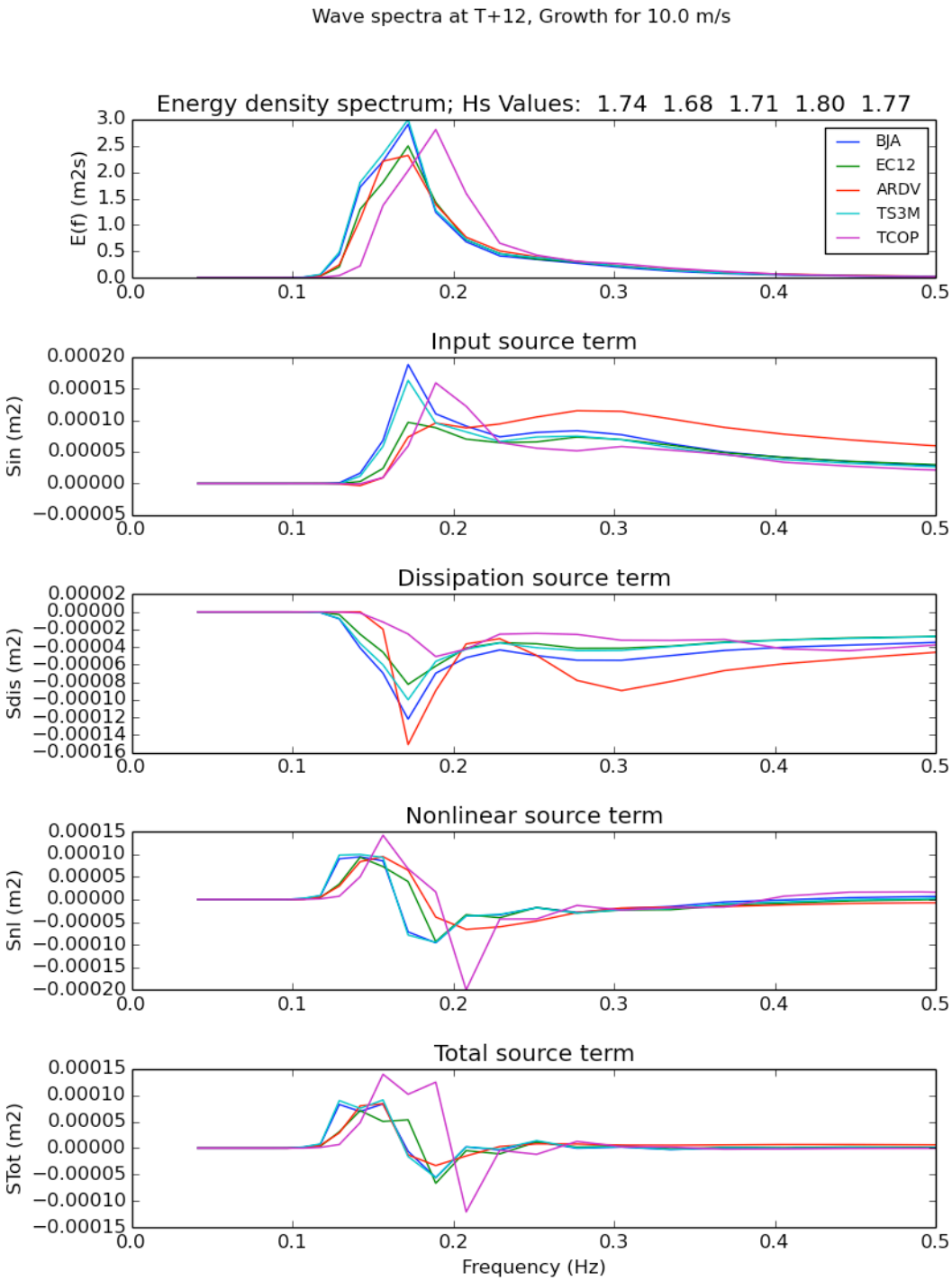

Figure 3.2. Wave spectra and source terms from growth test with constant wind speed at 10ms^{-1}. Model state after 12 hours forcing from calm.

© Crown copyright 2011

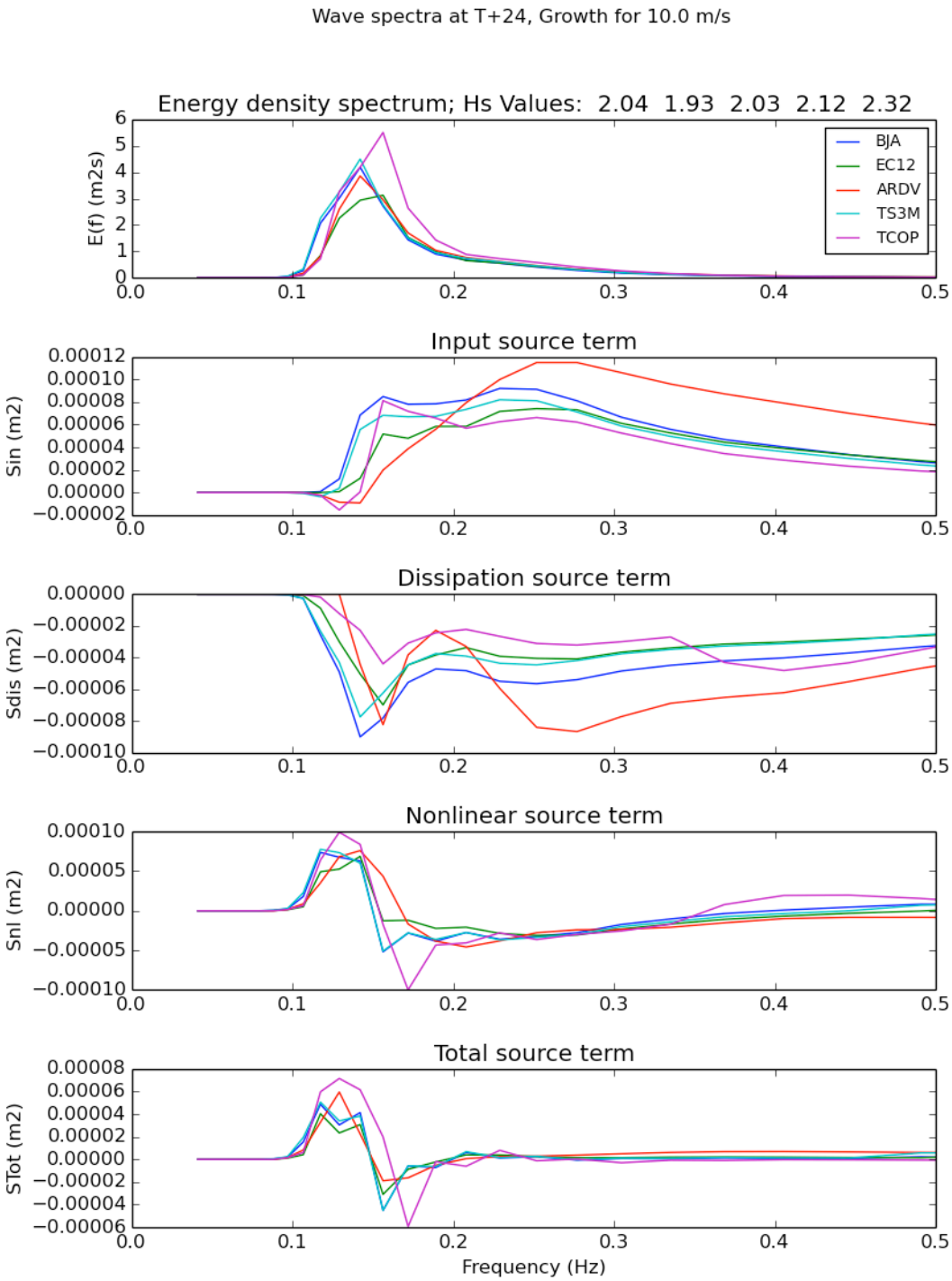

Figure 3.3. Wave spectra and source terms from growth test with constant wind speed at 10ms^{-1}. Model state after 24 hours forcing from calm.

© Crown copyright 2011

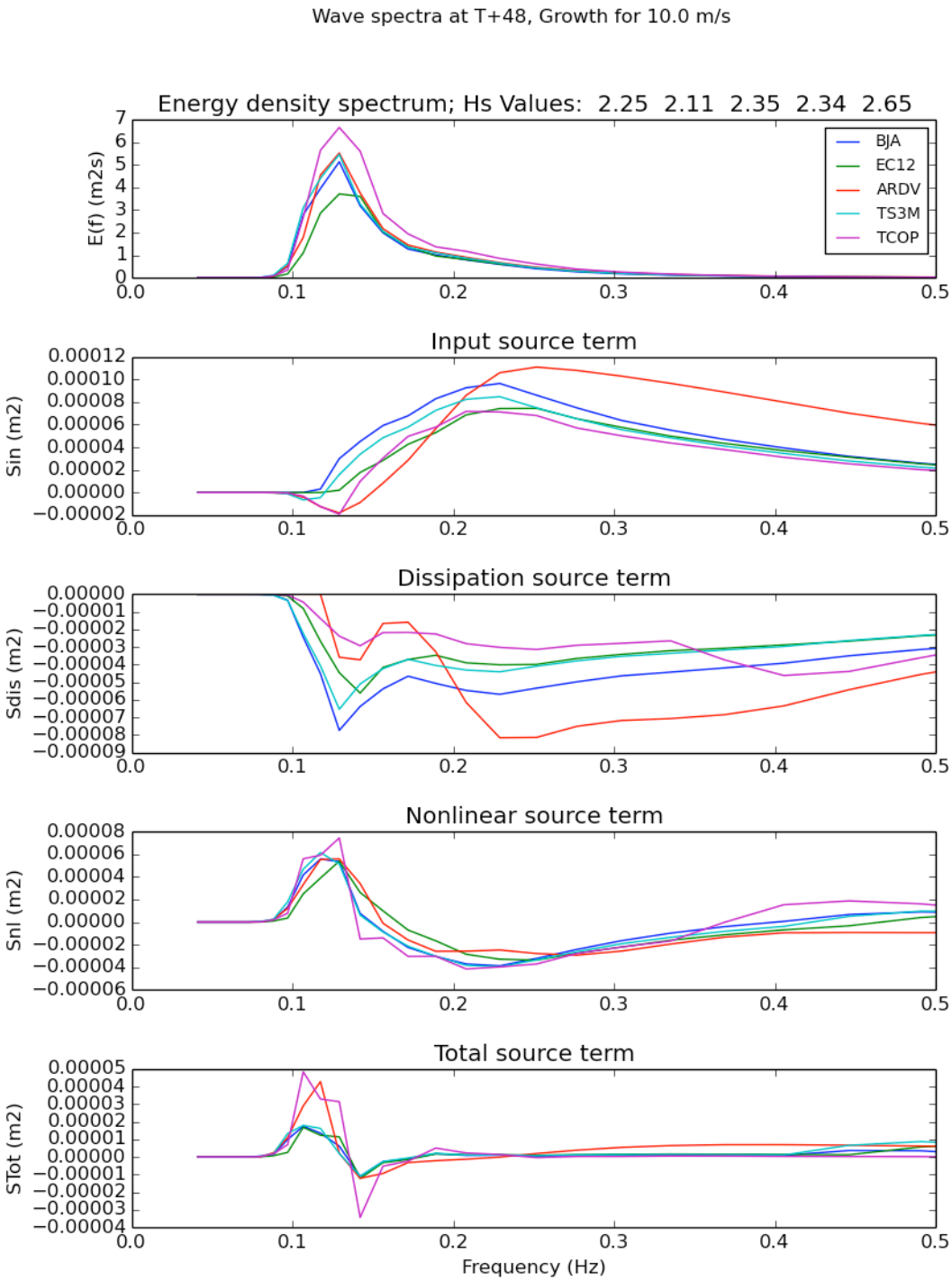

Figure 3.4. Wave spectra and source terms from growth test with constant wind speed at 10ms^{-1}. Model state after 48 hours forcing from calm.

© Crown copyright 2011

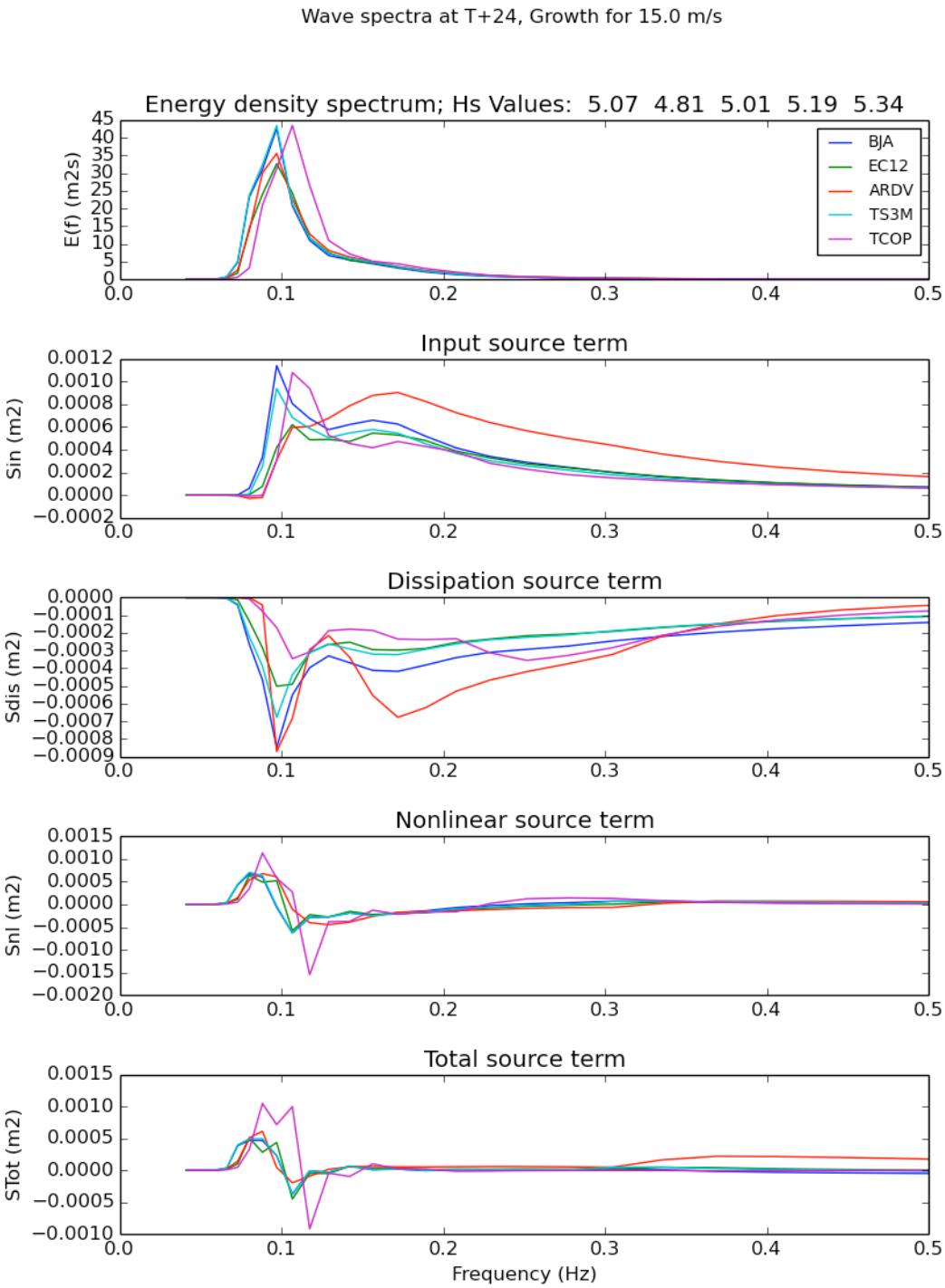

Figure 3.5. Wave spectra and source terms from growth test with constant wind speed at 15ms^{-1}. Model state after 24 hours forcing from calm.

© Crown copyright 2011

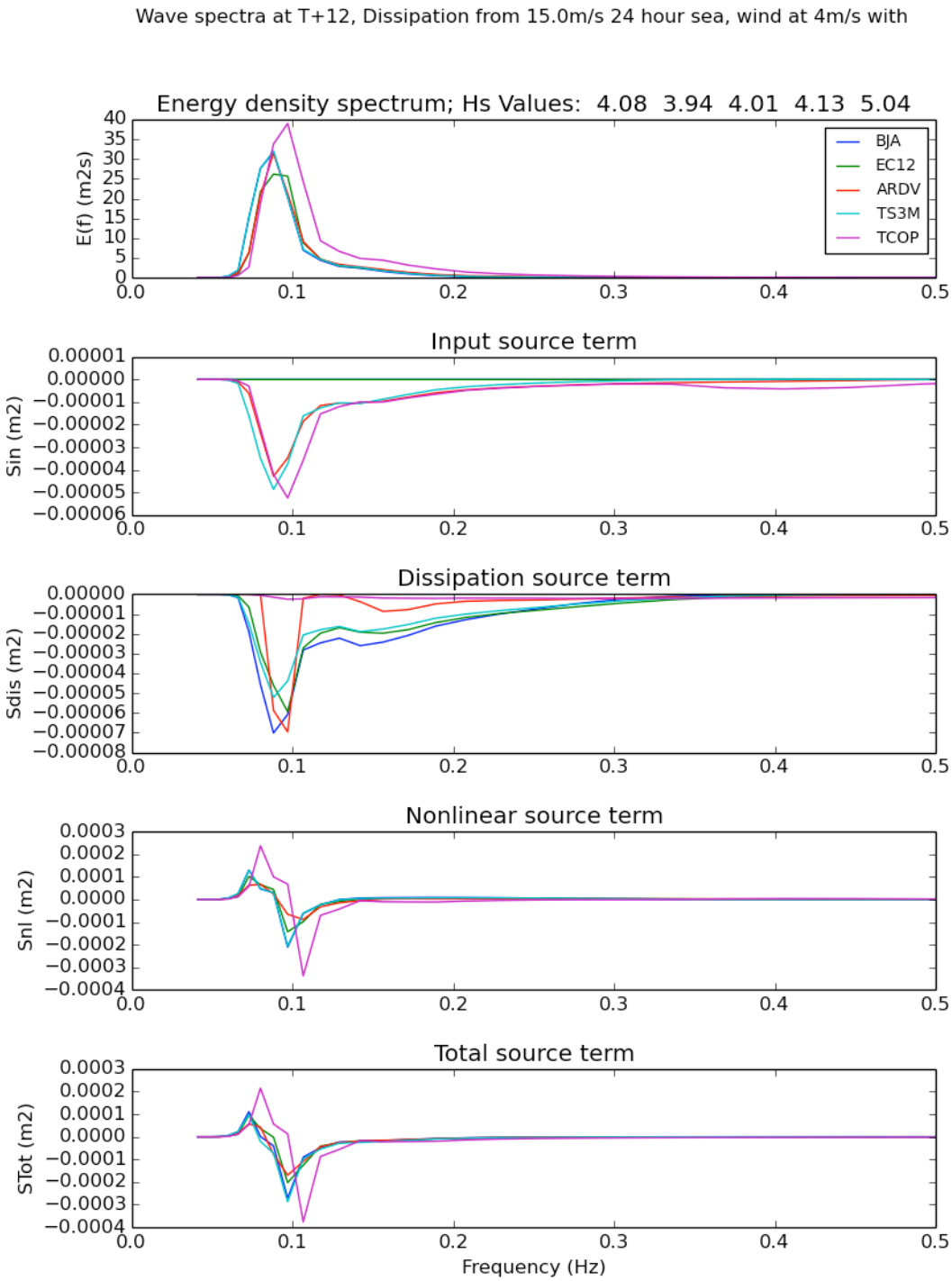

Figure 3.6. Wave spectra and source terms from dissipation test, with constant wind speed at 4ms^{-1} directed with the direction of wave travel. Model state 12 hours after the development of a 24 hour sea-state under a constant 15ms^{-1} wind (see Figure 6).

© Crown copyright 2011

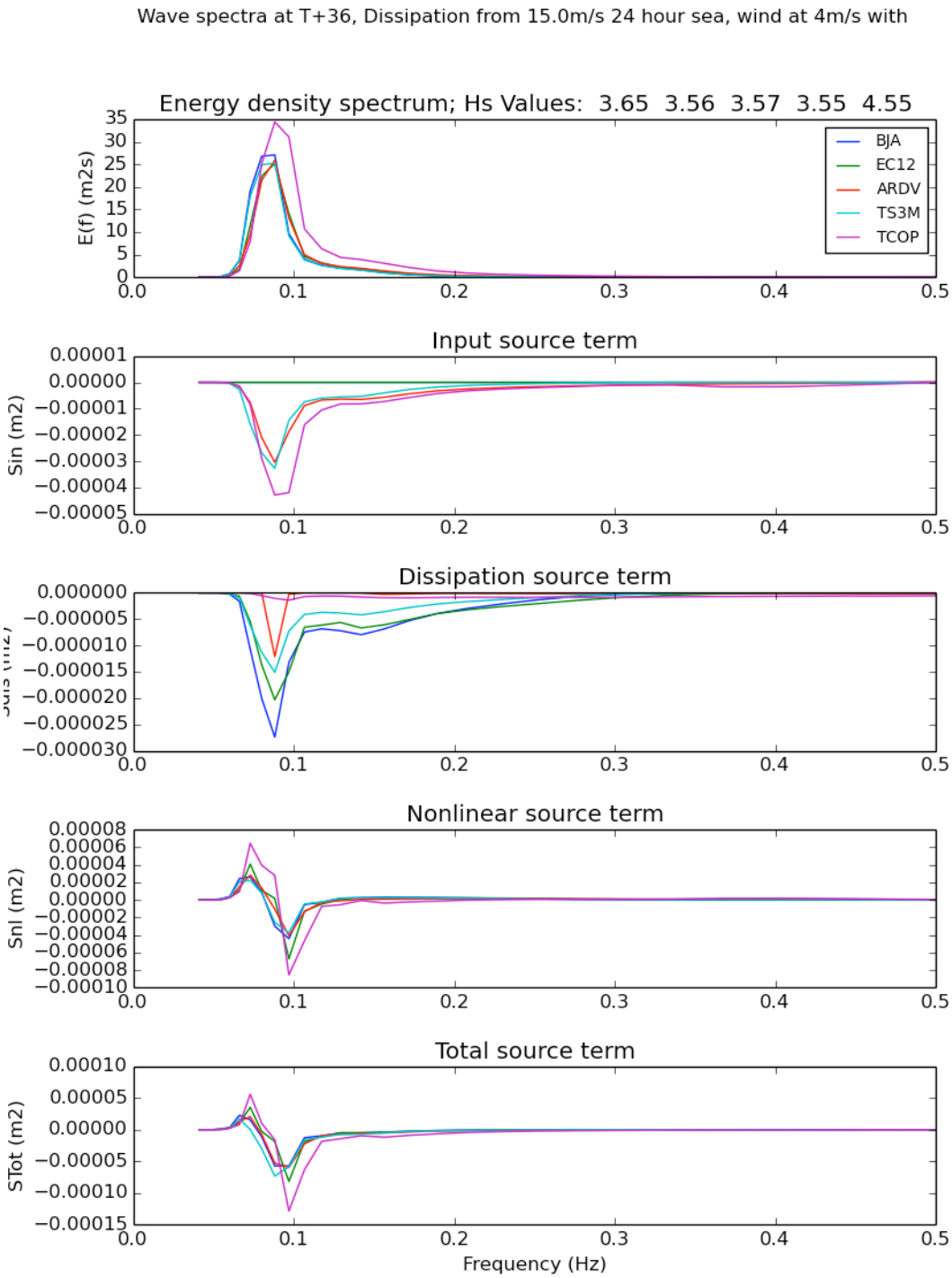

Figure 3.7. Wave spectra and source terms from dissipation test, with constant wind speed at 4ms^{-1} directed with the direction of wave travel. Model state 36 hours after the development of a 24 hour sea-state under a constant 15ms^{-1} wind (see Figure 6).

© Crown copyright 2011

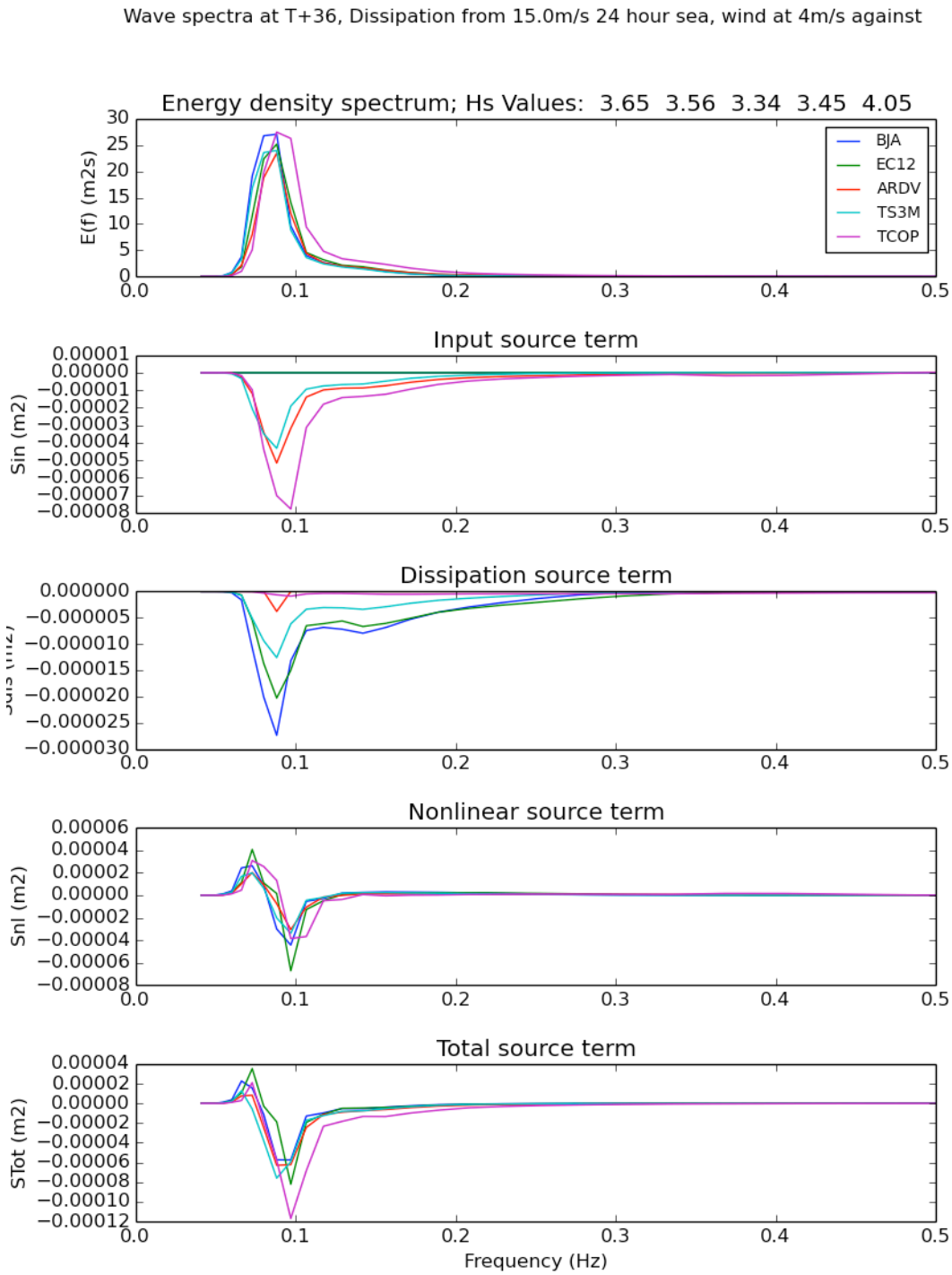

Figure 3.8. Wave spectra and source terms from dissipation test, with constant wind speed at 4ms^{-1} directed against the direction of wave travel. Model state 36 hours after the development of a 24 hour sea-state under a constant 15ms^{-1} wind (see Figure 6).

© Crown copyright 2011

4. Global wave model assessment

In general terms, the relative behaviours of the four different source terms can be described as follows:

- TCOP gives the slowest growth of young wind-sea, but will develop wave energy greater than the other source terms in very long fetches. The scheme is dissipative in swell dominated conditions (via a swell-atmosphere momentum transfer parameterisation).

- EC12 grows young wind-sea more rapidly than TCOP, but is the most constrained term for wave energy development in longer fetch situations. The scheme is weakly dissipative in swell dominated conditions.

- ARDV develops young wind-sea in a similar manner to EC12, but is less constrained in longer fetches. The scheme is dissipative in swell dominated conditions (as a function of both whitecapping and swell-atmosphere momentum transfer parameterisations).

- TS3M gives the most rapid growth of young wind-sea. This scheme is constrained for wave energy development in longer fetch situations, but at a higher 'ceiling' than for EC12. The scheme is the most dissipative in swell dominated conditions (as a function of both whitecapping and momentum transfer parameterisations).

In order to test how these behaviours translate in practise to the Met Office global wave model, a 1 year run of the model (for the year 2012) was made for each source term. Results were verified against both a remote sensed and in-situ observed baselines.

4.1 Global comparison with satellite altimetry

Spatial verification was undertaken by comparing the model runs against observations of Hs made by the Jason-2 satellite altimeter. The model-observation match up method was based on a 'model grid bin' scheme. In this method, successive altimeter soundings (equivalent to an approximately 7km along track sample of the ocean surface) were first referenced against the nearest model grid point in space and time (within a 1 hour window). Where, for each unique model grid point and time, 3 or more soundings

© Crown copyright 2011

were referenced, an average satellite Hs value was then calculated from the 3 closest soundings to the model point in order to generate a 'super-observation'. The super-observations were set at this scale in order to represent a sample of waves similar to that sampled by an in-situ observation. In order to achieve statistically robust data volumes for verification, the model versus super-observation match ups were further aggregated in 3 degree latitude by 4 degree longitude spatial bins.

Figure 4.1 illustrates the modelled wind forcing climate for the year 2012 runs. Model wind speeds (top panel) are strongest in high latitudes (with highest winds in the Southern Ocean) and the trade wind belts. Localised features, such as the Somali Jet, Tehuano wind (blowing offshore from the isthmus of Tehuantepec) and strengthening winds in the Caribbean, can be identified. An estimate of wave age (based on the ratio between wave phase speed and wind speed, bottom panel) illustrates the main areas for young wind-sea development (low wave age) and swell dominated conditions (high wave age). Although one might expect some increase in wave age toward the 'fetch end' of the main storm tracks, the links between regions of strong wind forcing and low mean wave age appear very strong.

Figure 4.2 shows the data sample size and (annual) mean Hs values for each of the 3x4 degree spatial verification bins. Sample sizes are generally greater than 600 data values. The highest mean wave heights are associated with long fetches in the main high latitude storm tracks.

Figures 4.3-4.6 show the spatial distribution of (model minus observed) Hs bias, root mean squared error normalised by observed mean Hs (NRMSE) and the ratio between model and observation standard deviation (NSD). The bias statistic (ideal value 0.0) is used to show the effect of the different physics choices on the overall average wave energy developed by each model. NRMSE indicates the reliability of the model (ideal value 0.0) and can be used to identify regions of the model where predictive skill might be expected to be limited (e.g. around SE Asia and Indonesia for all the schemes). NSD is used to indicate the resolution of the model, i.e. the degree to which any time varying signal in the model replicates that in the observations. It is worth noting that observed variability comprises both the true variability of Hs plus a component of observational error, so an ideal value for NSD is just less than 1.0.

© Crown copyright 2011

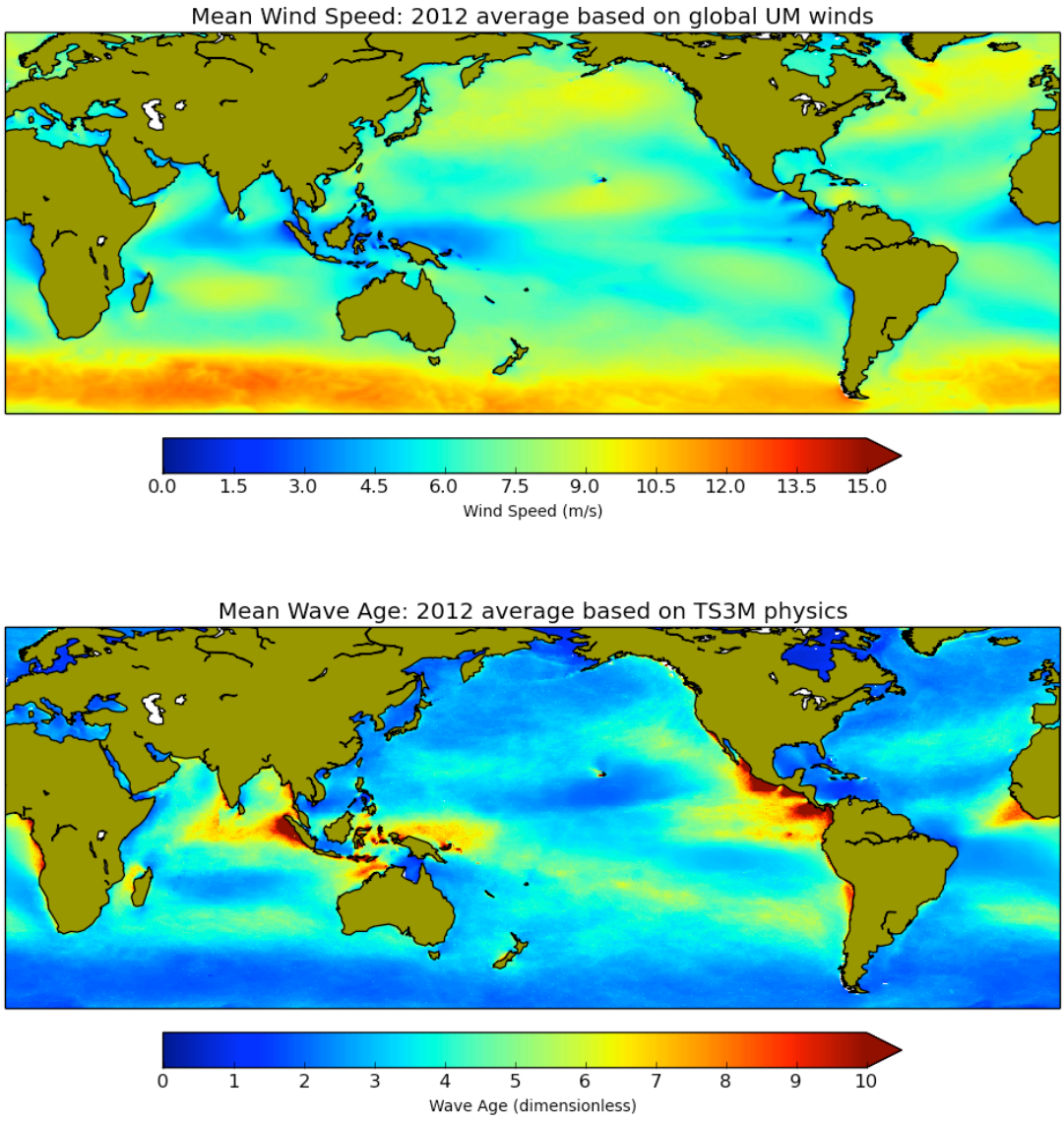

Figure 4.1. (Top panel) Mean wind speed (ms^{-1}) and wave age data (lower panel) from the 2012 trial period. Wave age is defined as the ratio between (peak period derived) wave phase speed and wind speed – high values will demark areas where long range swell and light wind conditions predominate, low values where growing wind-seas predominate.

© Crown copyright 2011

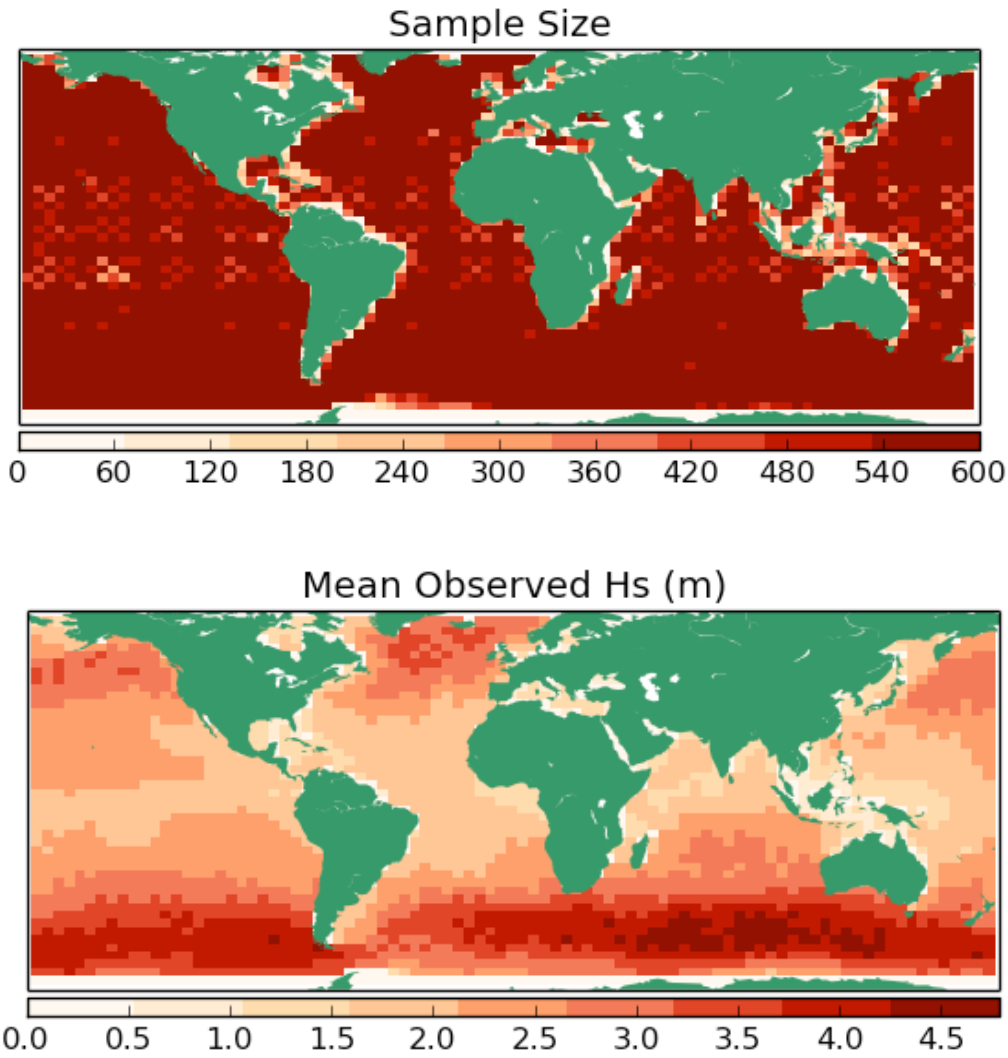

Figure 4.2. (Top panel) Number of matched model-observation pairs and (lower panel) observed mean significant wave height from JASON-2 altimeter during 2012. For analysis purposes, data are binned geographically into 3 degree latitude by 4 degree longitude cells.

Figure 4.3 shows the results for TCOP. The main features are a generally positive bias, NRMSE less than 0.16 for the majority of mid-high latitude cells, and a general overestimation of the observed variability. Examining the bias in more detail, the figure shows a west-east gradient in bias in the northern hemisphere storm tracks. This implies that wave energy is under-predicted in developing wind-sea areas at the west end of a storm track and over-predicted at the east end, when wind-seas might be expected to be more mature. Positive bias is strong in the Southern Ocean, where fetches can be particularly long. For the swell dominated regions (identified in Figure

© Crown copyright 2011

4.1), Figure 4.3 shows that TCOP has a neutral or low bias. NRMSE appears particularly good in regions just downwind of the trade wind belts.

Figure 4.4 shows the results for EC12. In terms of spatial distribution, the verification is significantly different to the TCOP results. Bias is more evenly distributed between positive and negative values and, whilst a west-east gradient can still be detected, the main geographic demarcation in bias occurs between the high latitude storm tracks (negative or neutral bias) and swell dominated regions (positive bias). NRMSE for the EC12 run is generally lower in the storm tracks than for TCOP, but is higher in swell dominated regions. More striking is the overall lower level of NSD for EC12 compared to TCOP, particularly in low latitudes. Considering Figures 4.3 and 4.4 together, the results appear consistent with the relative behaviours of the two source term schemes. For example the more marked west-east gradient in TCOP can be attributed to that term's development of wind-sea. The behaviour of EC12 in swell dominated regions, including the low levels of variability in the tropics, may be attributed to the lack of an explicit swell dissipation parameterisation.

ARDV and TS3M have attributes of both the TCOP and EC12 schemes. Figure 4.5 shows the ARDV results. Bias is not as strongly positive as for TCOP, but still shows a significant west-east gradient in the northern hemisphere storm tracks and a positive bias in the Southern Ocean. Ardhuin et al. (2010) attributed at least some of the Southern Ocean bias to the lack of a parameterisation for icebergs. Low positive, or neutral, biases in swell dominated regions suggest a slightly weaker swell dissipation than for TCOP. This may also be the cause of the lower levels of variability (NSD) in the tropics when ARDV is compared to TCOP. In higher latitudes the NSD for ARDV is significantly closer to 1.0 than for TCOP. Overall the ARDV NRMSE statistics are generally lower than for TCOP, particularly in high latitudes. High latitude NRMSE values are similar to EC12 and ARDV performs better than EC12 in swell dominated regions.

In principle, TS3M is the most active of the four schemes, both in terms of wind-sea development and dissipation under swell dominated conditions. Figure 4.6 shows results from the TS3M run. TS3M Hs values are generally biased slightly low, particularly in the southwest sector of the North Atlantic and the western part of the Indian Ocean. In the northern hemisphere storm tracks the model is biased slightly negative, or neutral, with a limited west-east gradient. The Southern Ocean is biased

© Crown copyright 2011

slightly high. Overall, NRMSE statistics follow a similar pattern to ARDV, as does NSD, although the TS3M run has slightly higher variability in the subtropics.

The differences in bias between TS3M and ARDV may be explained by considering a) the climate of wave generation in the oceans and b) the role of the dissipation in TS3M. From the analysis of wave growth in Section 2, TS3M might be expected to generate higher waves than ARDV for storms that develop and are maintained over 12-36 hour periods. Subsequent to the storm, TS3M will more actively diminish wave energy via both its whitecapping and swell dissipation processes. The ARDV scheme will develop wave heights similar to TS3M over a long fetch and lead time (e.g. Figure 2.4). Whilst storms are a regular feature of the high latitudes, a general west-east development of waves under more moderate conditions (either by ocean scale wind fields set up under slowly developing large atmospheric circulation systems, or when waves travelling west-east are forced by successive storms) will make up a substantial component of the climate. West-east gradients in the TCOP and ARDV bias maps suggest that these processes make a contribution to the overall climate similar to that made by more energetic, rapidly moving, storms. Such a gradient is not prominent in the TS3M run, for which the most rapid development of wave energy occurs when young wind-seas are 'spun up'. The regions where negative bias is noted for TS3M correspond to locations with moderately high wave age, just downwind of a storm track, suggesting that the initial dissipation of wind-sea, once forcing winds diminish, may be too high in TS3M.

Although overall bias is slightly negative, or neutral, the rapid development of waves in TS3M means that the model is good at capturing particularly high waves associated with deep lows formed in the northern hemisphere storm tracks. This is demonstrated by the quantile-quantile plots in Figure 4.7 and in figures in Section 4.2. High wave prediction is considered particularly important for a model with a primary role of warning mariners about extreme conditions. TS3M was also found to be the best performing system in an overall comparison of the results of in-situ verification of the four schemes. For these reasons, plus the consistency that TS3M has with the EC12 scheme (presently adopted for Met Office regional models), TS3M was selected as the favoured scheme for operational implementation in the global wave model. The remaining verification in this document will focus on the behaviour of TS3M as the replacement for TCOP.

© Crown copyright 2011

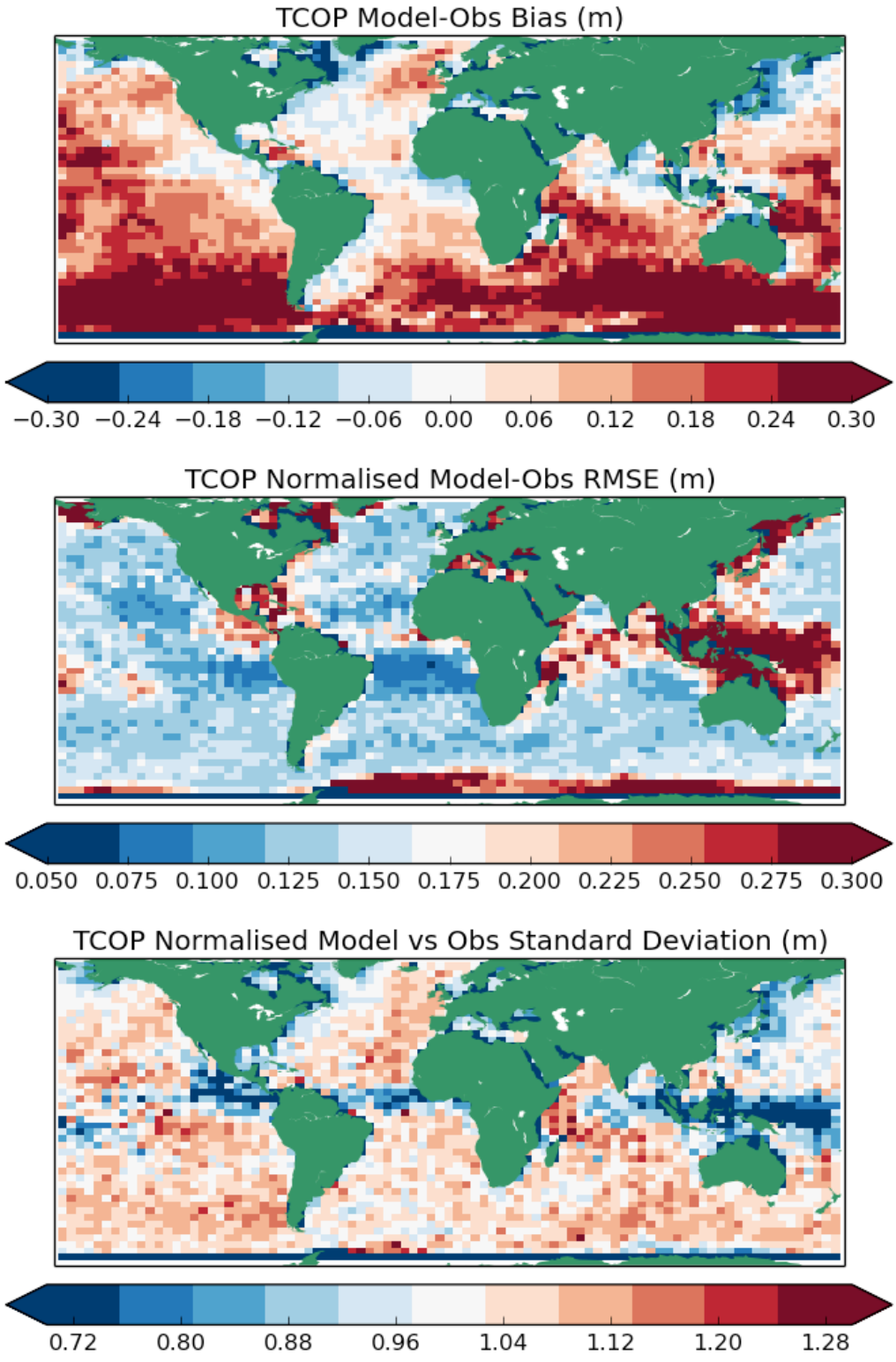

Figure 4.3. Significant wave height (Hs) verification against JASON-2 satellite altimetry for the TCOP run. (Top panel) Model minus observation bias, (middle panel) Root Mean Squared Error normalised by observed Hs, (lower panel) model Hs standard deviation normalised by observation Hs standard deviation.

© Crown copyright 2011

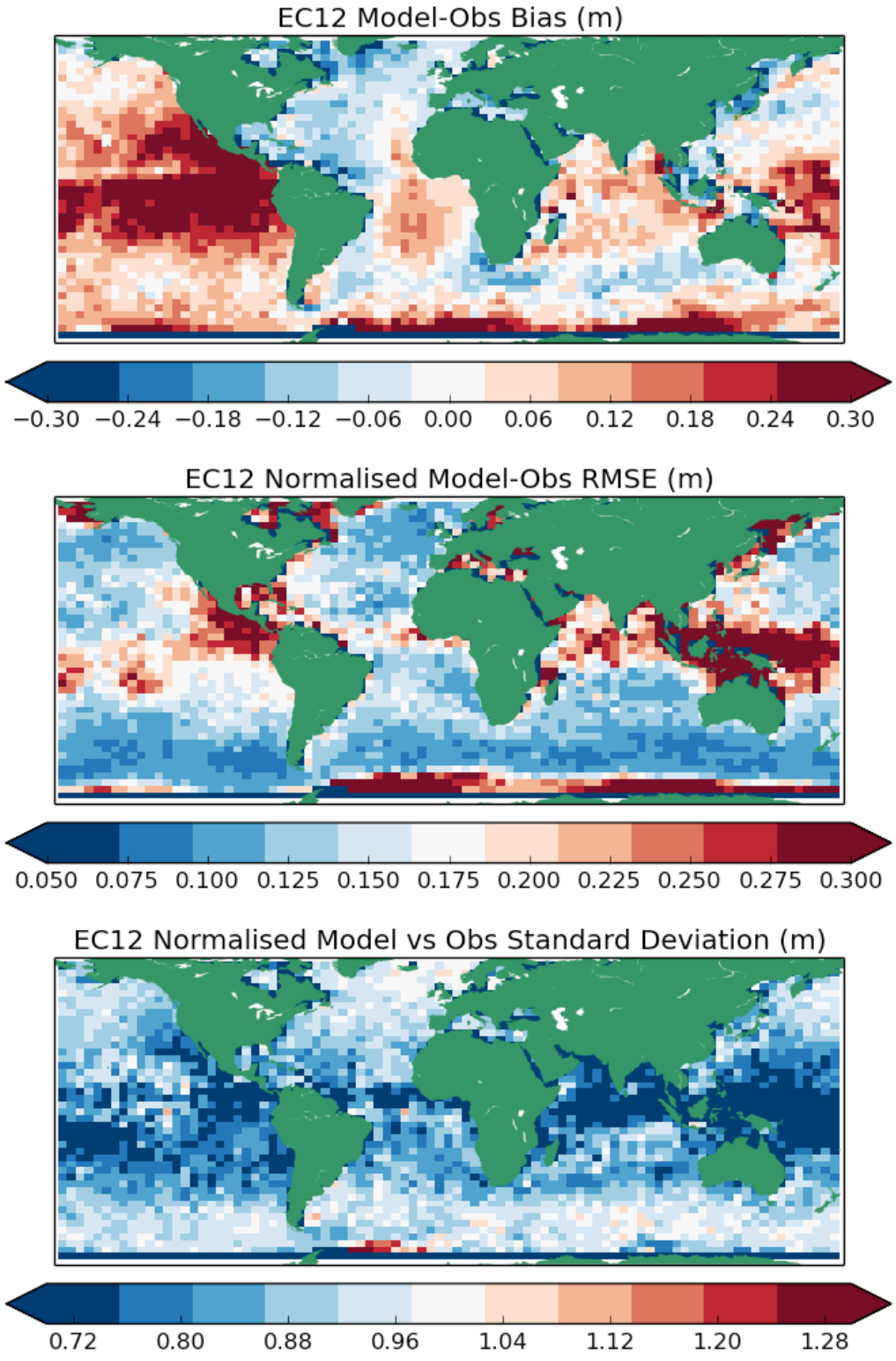

Figure 4.4. Significant wave height (Hs) verification against JASON-2 satellite altimetry for the EC12 run. (Top panel) Model minus observation bias, (middle panel) Root Mean Squared Error normalised by observed Hs, (lower panel) model Hs standard deviation normalised by observation Hs standard deviation.

© Crown copyright 2011

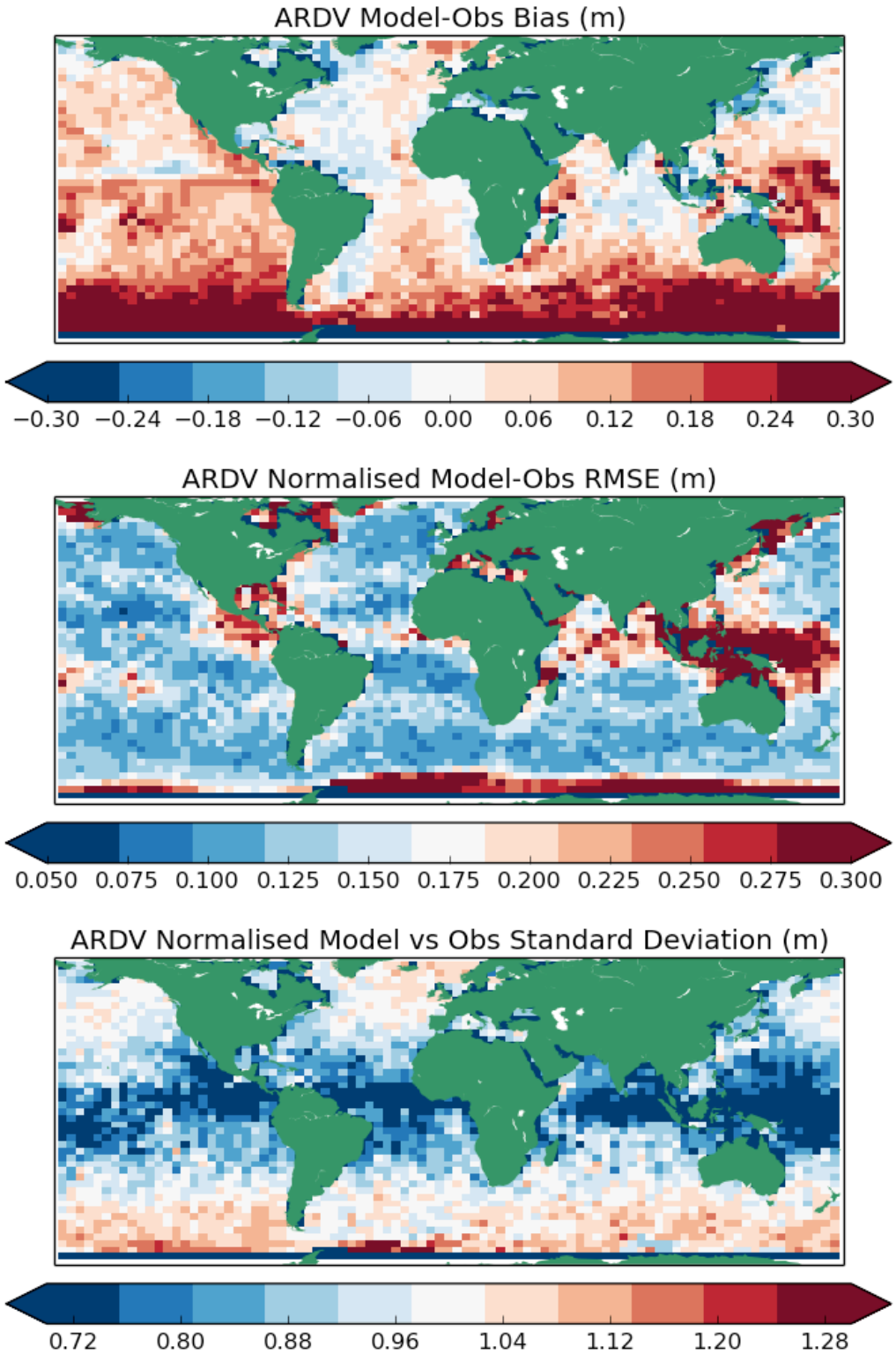

Figure 4.5. Significant wave height (Hs) verification against JASON-2 satellite altimetry for the ARDV run. (Top panel) Model minus observation bias, (middle panel) Root Mean Squared Error normalised by observed Hs, (lower panel) model Hs standard deviation normalised by observation Hs standard deviation.

© Crown copyright 2011

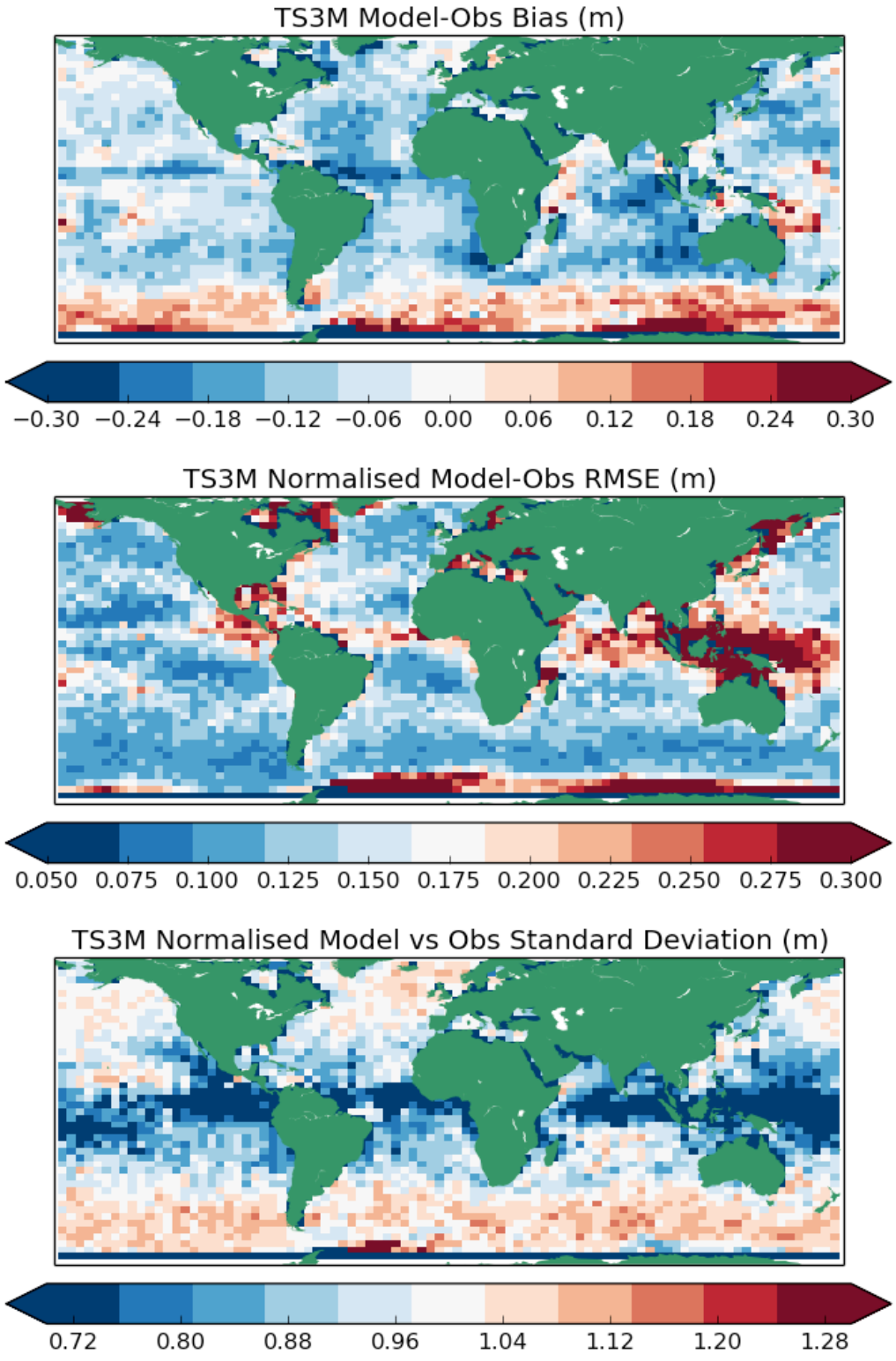

Figure 4.6. Significant wave height (Hs) verification against JASON-2 satellite altimetry for the TS3M run. (Top panel) Model minus observation bias, (middle panel) Root Mean Squared Error normalised by observed Hs, (lower panel) model Hs standard deviation normalised by observation Hs standard deviation.

© Crown copyright 2011

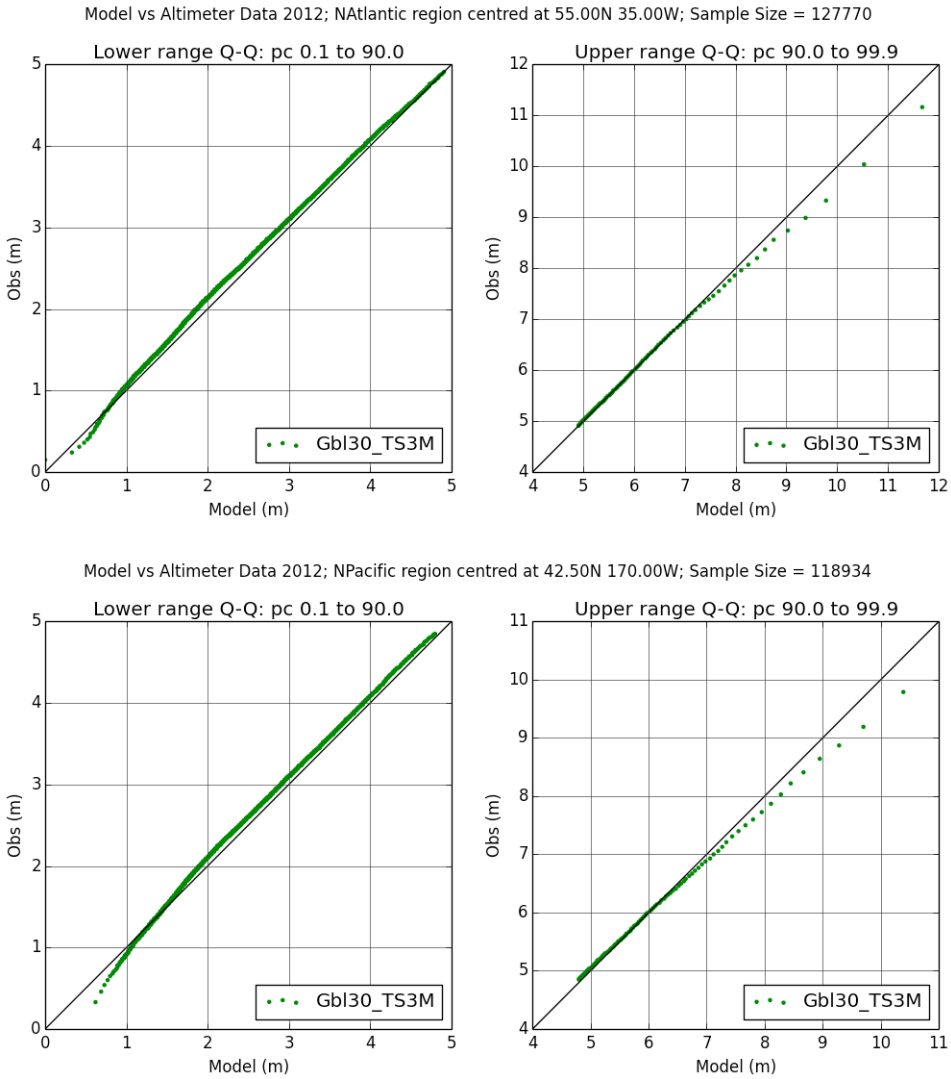

Figure 4.7. Significant wave height quantile-quantile plots for TS3M run model-altimeter match-ups in (top panel) the North Atlantic (40N, 70W to 70N, 0W) and (bottom panel) the North Pacific (30N, 150E to 55N, 130W). Left hand side plots show quantiles 0.1-90.0%, right hand side plots show quantiles 90.1 to 99.9%.

4.2 Regional comparison with in-situ observations

The 2012 runs were compared with in-situ data available to the Met Office via the WMO-IOC Joint Commission for Marine Meteorology (JCOMM) 'Intercomparison of Operational Wave Forecast Models', operated by ECMWF. Details of the intercomparison project can be found in Bidlot et al. (2002, 2007). Observation data are

© Crown copyright 2011

quality controlled following Bidlot et al. (2002) and made available as both an 'instantaneous observation' and a 'super-observation' over a 4 hour time window. In the analysis here, the instantaneous data were used, since these provide a better representation of the errors that a marine user will see if they compare model and observations in real-time. Observed values for Hs, peak period (Tp) and mean zero-upcrossing period (Tz) were used in the verification. Figure 4.8 shows a map of the in-situ observation locations, which encompass a range of platform and instrument types. The main features of platform location are a general proximity to land and a high number of platforms in the northern hemisphere. In the verification, a sample using all platforms was analysed, but further sub-sampling was conducted in order to assess the performance of the model runs in different regions.

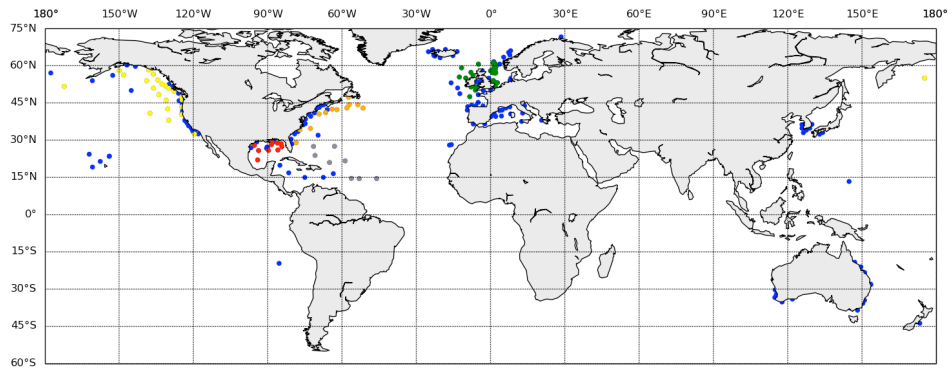

Figure 4.8. Locations of in-situ data platforms used for verification. Subset regions discussed in subsequent figures are marked as Northeast Pacific (yellow), Gulf of Mexico (red), UK (green), Caribbean-Atlantic (grey), Northwest Atlantic (orange).

Verification in subsequent figures are presented using a 6-panel plot comprising:

1. Top left – parameter distributions plus summary statistics for the observations and two model runs.
2. Top right – model minus observation bias and standard deviation/RMSE data. The plots compare model run statistics through the prediction range (using overlapping 5% subsamples of the data), whilst the text gives an overall statistic.

© Crown copyright 2011

3. Centre left – quantile-quantile (q-q) distribution of model minus observation errors for the two runs, plus summary statistics for the error distributions.
4. Centre right – Taylor plot for the two model runs, plus a linear fit relationship between observations and model.
5. Bottom left – Model versus observation q-q plot for the lower 90% of conditions.
6. Bottom right – Model versus observation q-q plot for the upper 10% of conditions.

The assessment of model quality is based on a holistic view of this group of metrics.

Figure 4.9 shows the comparison, for all in-situ Hs data, between TCOP and TS3M. For this overall sample there is little to discriminate the two runs. However, TS3M yields a slightly (5%) lower RMSE than TCOP and has slightly lower under-prediction errors at the extremes (where the lower tail of the q-q distribution departs from the 1:1 line in plot 3). The main difference is in the profile of the bias through prediction range in plot 2. Both models are biased negative when forecasting low wave heights and biased positive when predicting wave heights in the upper quantiles. However, whilst TS3M is neutrally biased through much of the prediction range, TCOP is biased positive above approximately 1.8m. Unless a model is perfectly correlated with the observations, the negative and positive 'kinks' in bias at the predicted range tails are to be expected (since observations will not be distributed evenly in the tails), but a majority of the bias profile should be neutral, so TS3M falls closer to the ideal behaviour than TCOP.

More variability can be seen in the performance of the two models when the verification is broken down into regions. Figure 4.10 assesses the Gulf of Mexico, where waves are generally benign (less than 2m for 90% of the time), but higher waves can be generated by extra-tropical storms. TS3M has a slight negative bias overall, but has lower RMSE, due to a slightly better level of correlation with observations than TCOP (plot 4), and appears to be better at replicating wave heights in the very upper quantiles (plot 6).

Figure 4.11 assesses the Northeast Pacific, where the wave age climate is moderate-high. TS3M shows a significant under-prediction bias (plots 2, 3 and 5) but has better RMSE and correlation (plots 2 and 4). The improvement in correlation is probably associated with a better capture of higher wave conditions (plots 2 and 6). Extreme under-prediction errors are lower for TS3M than for TCOP in this region (plot 3).

The Caribbean-Atlantic region (Figure 4.12) was one where the satellite verification showed a substantial negative bias for TS3M. In this region, TS3M clearly performs worse than TCOP, with increased RMSE (plot 2) and a noticeable bias in the error q-q

© Crown copyright 2011

plot (plot 3). Variability in the observations is under-represented by TS3M (plot 4), although the scheme may well generate higher waves associated with the most extreme storms as well as, or better than, TCOP (plot 6, for 99.5% quantile and above).

TS3M shows more favourable performance where observations are made in or close to storm tracks (Figures 4.13 and 4.20-21). Figure 4.13 assesses the performance at the west end of the North Atlantic storm track, where development of young wind-sea is a regular feature of the wave climate. The most striking feature is the ability of TS3M to replicate wave heights at higher quantiles (plot 6) relative to TCOP. This behaviour is likely to be tied to a reduction in the size of the largest under-predcition errors (plot 3) and reduction in overall bias for TS3M. TS3M RMSE statistics are improved over the TCOP value by approximately 4%.

Figures 4.14 and 4.15 verify Tp for, respectively, all available observations and data in the region of the UK. Tp is a relatively unstable parameter to verify and, in this case, the verification is not helped by truncation of observations to the nearest second at a large number of stations. Globally, Tp is estimated with poor skill by both schemes. TS3M performs the worst, by virtue of a positive bias in higher conditions and higher variability relative to TCOP. However, performance of the two schemes is more skilful and much closer around the UK. In this region TS3M better represents the upper quantiles of the Tp distribution and has an overall bias closer to zero. Figures 4.16 and 4.17 show the same analyses for Tz. In these cases, bias, RMSE and replication of the Tz distribution are generally better for TS3M. Indeed, Tz RMSE is improved by 10% globally and 13% for waters around the UK.

© Crown copyright 2011

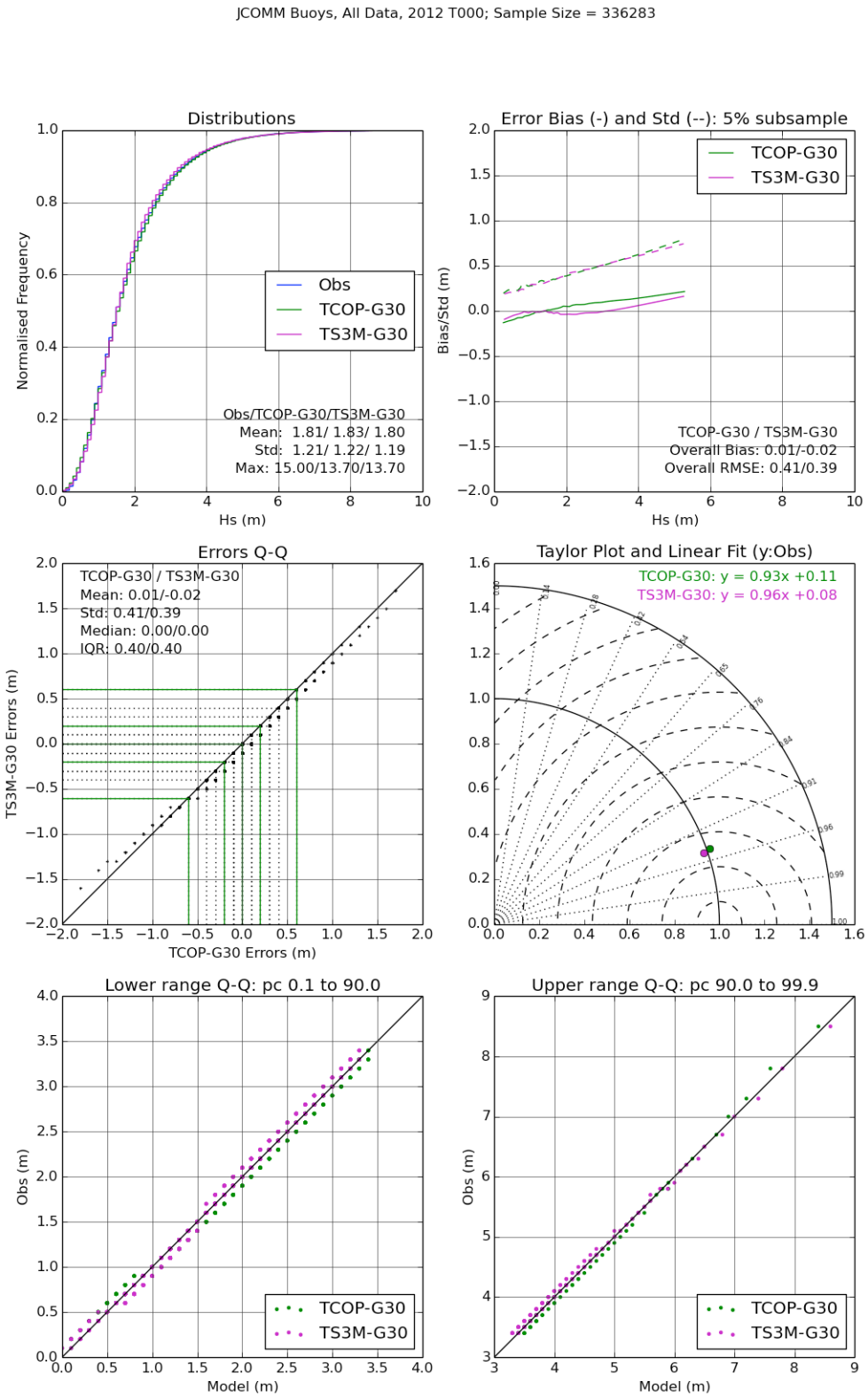

Figure 4.9. Significant wave height (Hs) verification against in-situ platforms for the TCOP and TS3M runs of the Global wave model. Statistics based on all available data.

© Crown copyright 2011

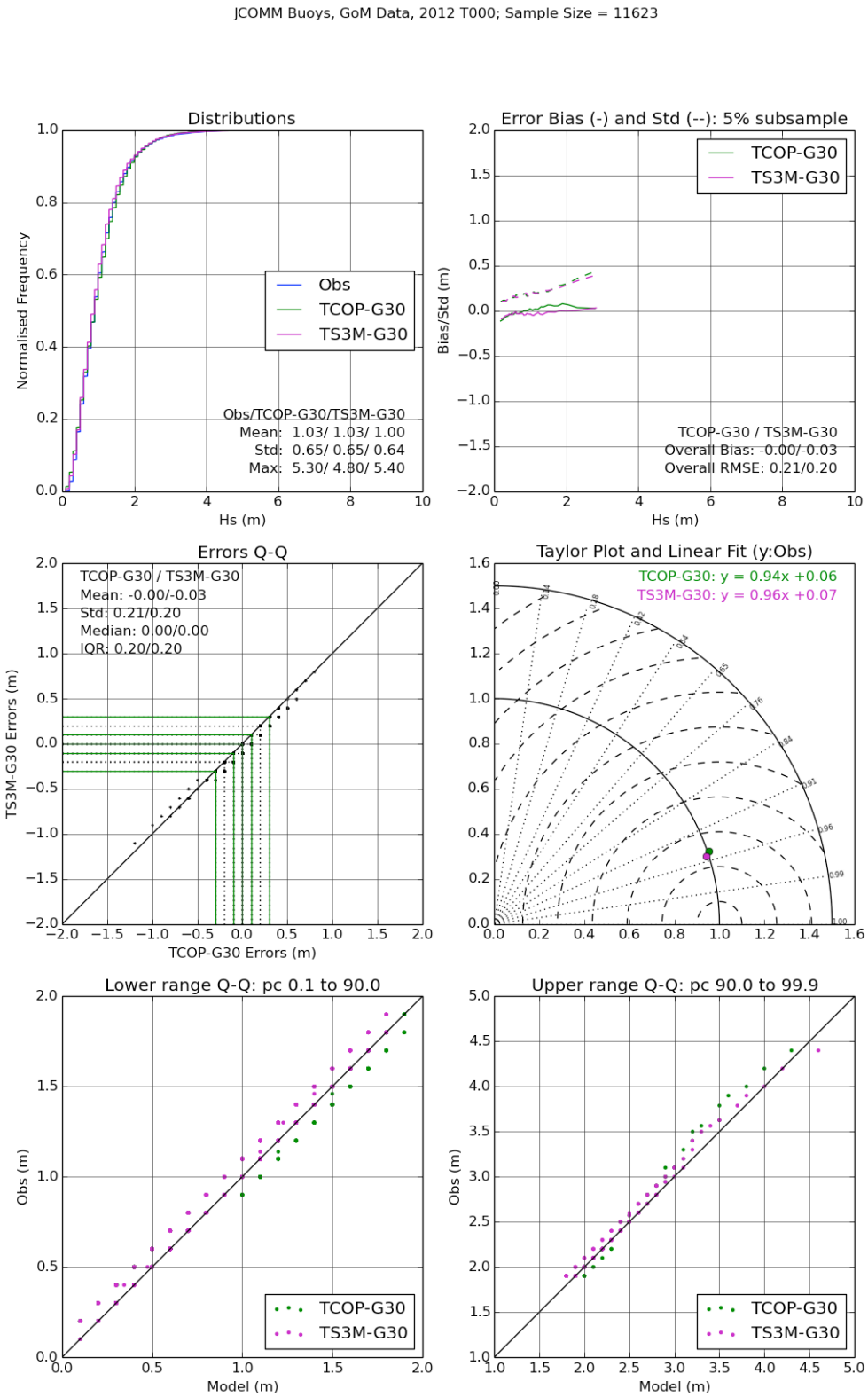

Figure 4.10. Significant wave height (Hs) verification against in-situ platforms for the TCOP and TS3M runs of the Global wave model. Statistics for Gulf of Mexico region.

© Crown copyright 2011

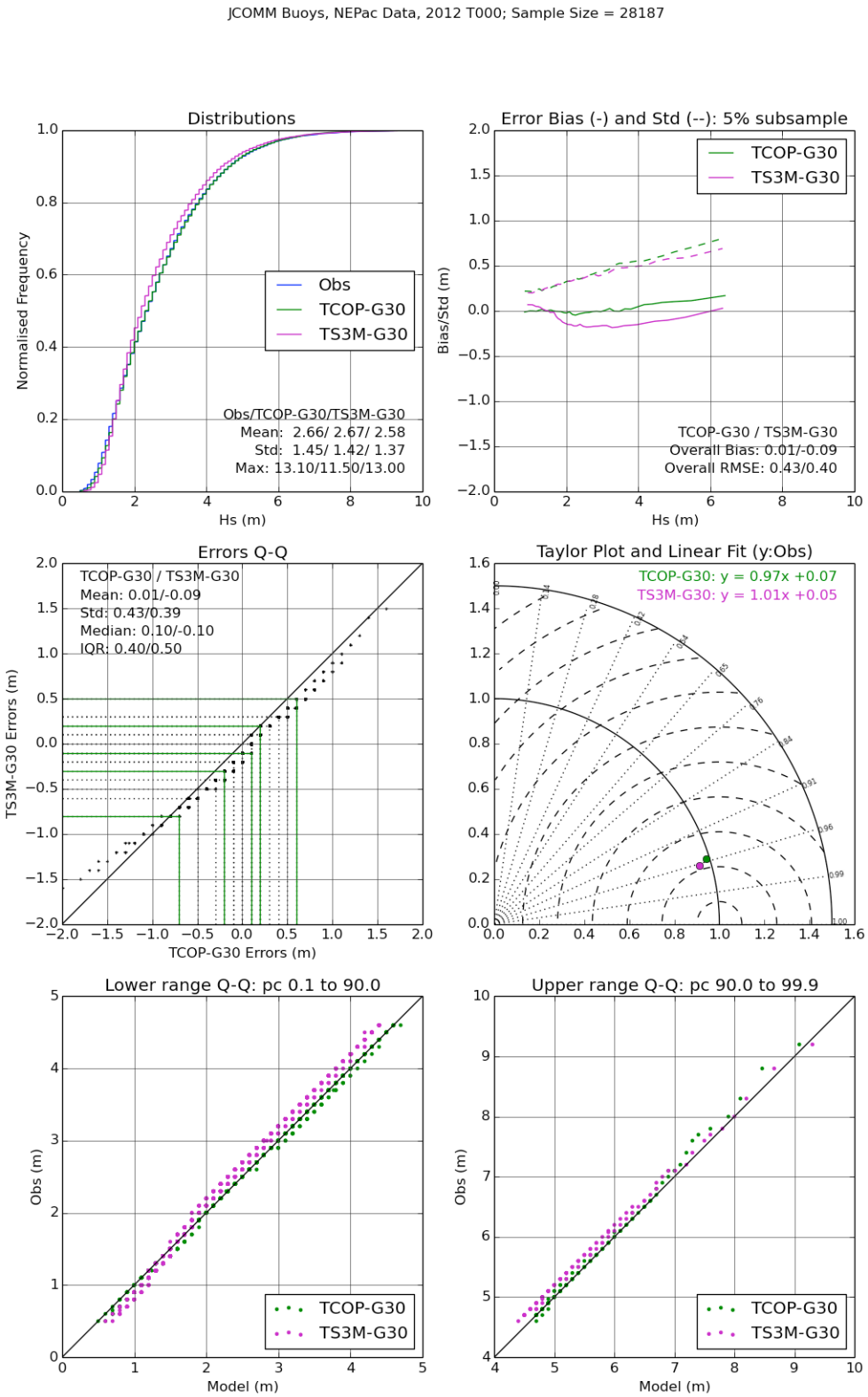

Figure 4.11. Significant wave height (Hs) verification against in-situ platforms for the TCOP and TS3M runs of the Global wave model. Statistics for northeast Pacific.

© Crown copyright 2011

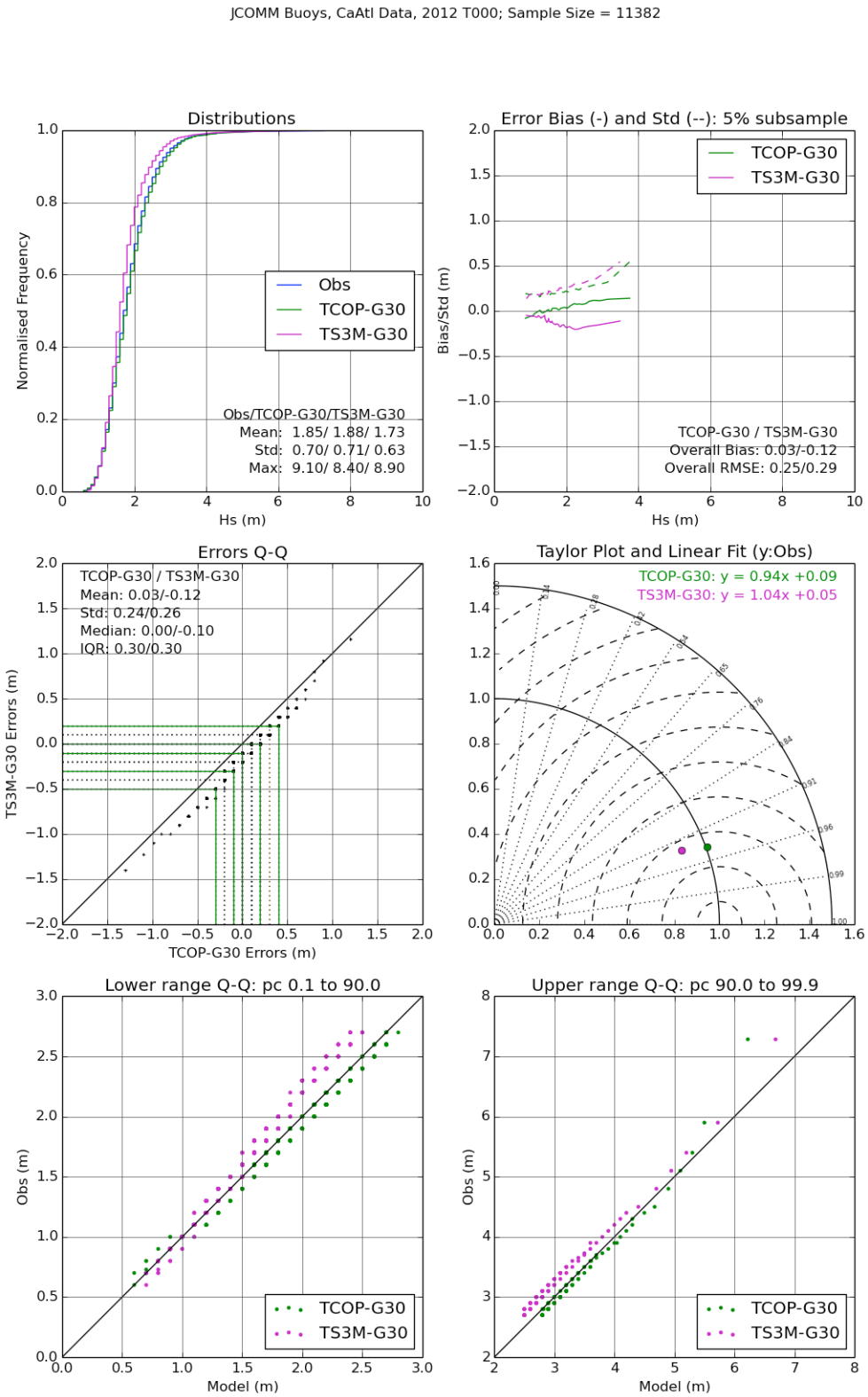

Figure 4.12. Significant wave height (Hs) verification against in-situ platforms for the TCOP and TS3M runs of the Global wave model. Statistics for Caribbean-Atlantic region.

© Crown copyright 2011

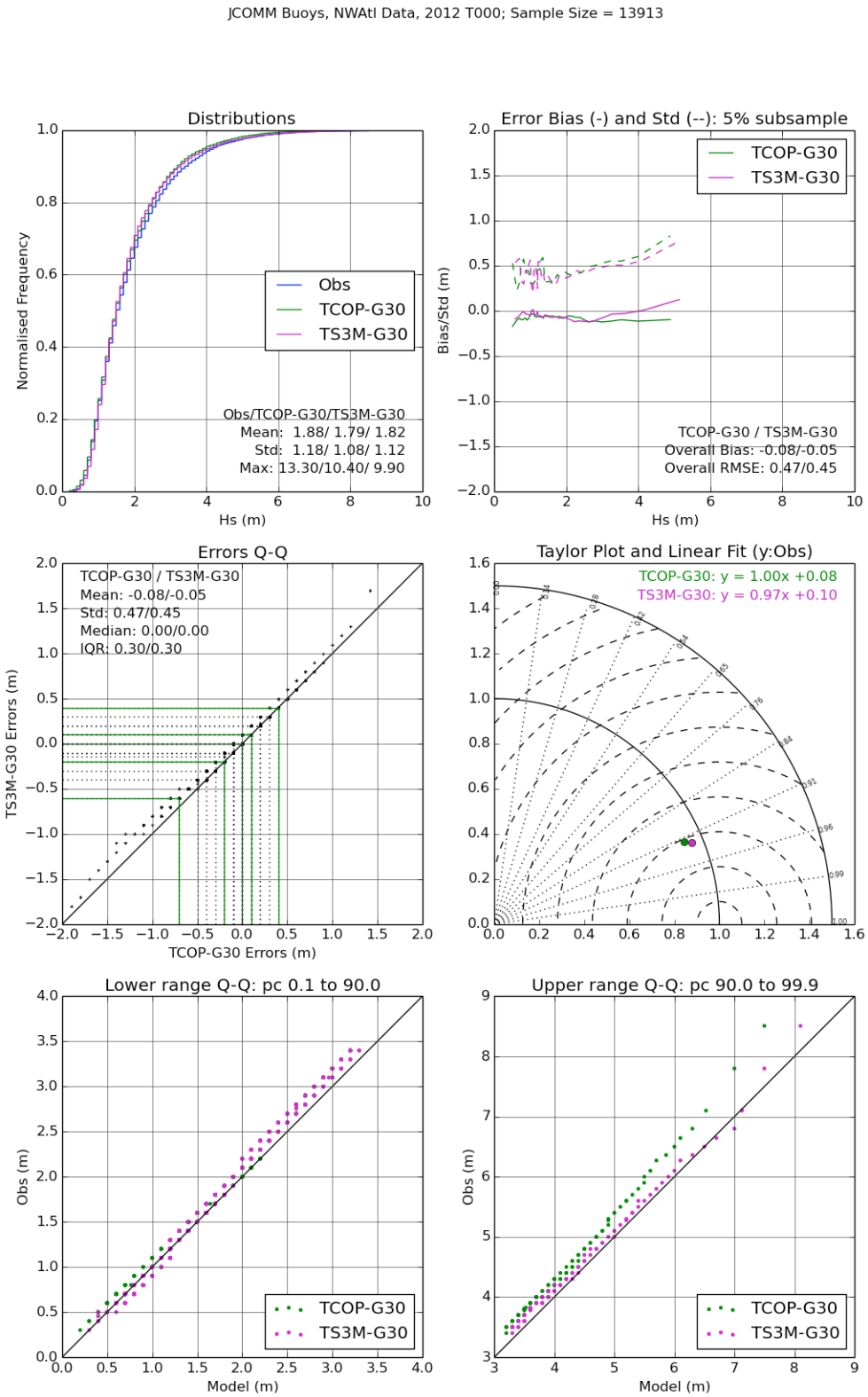

Figure 4.13. Significant wave height (Hs) verification against in-situ platforms for the TCOP and TS3M runs of the Global wave model. Statistics for northwest Atlantic region.

© Crown copyright 2011

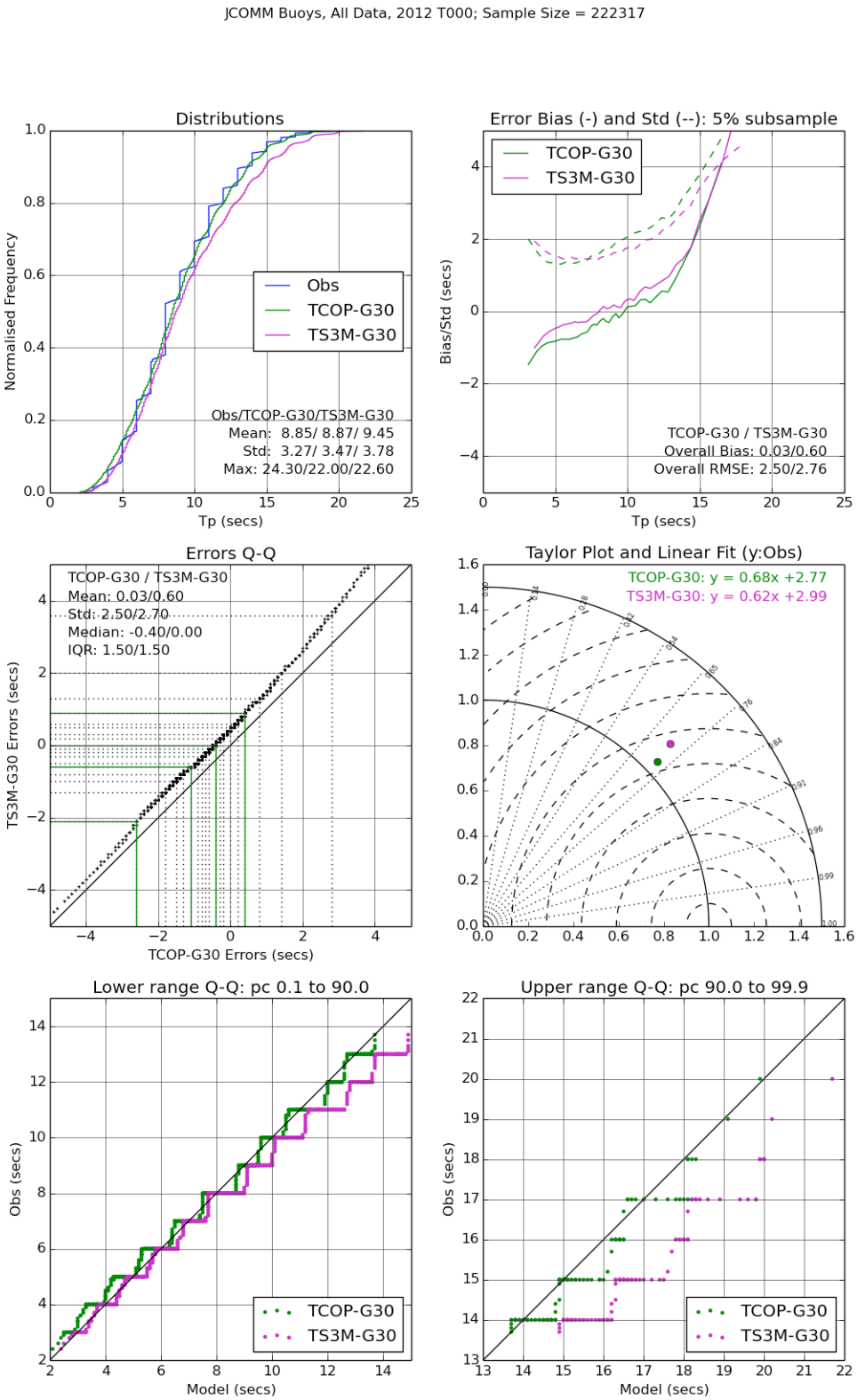

Figure 4.14. Peak period (Tp) verification against in-situ platforms for the TCOP and TS3M runs of the Global wave model. Statistics based on all available data.

© Crown copyright 2011

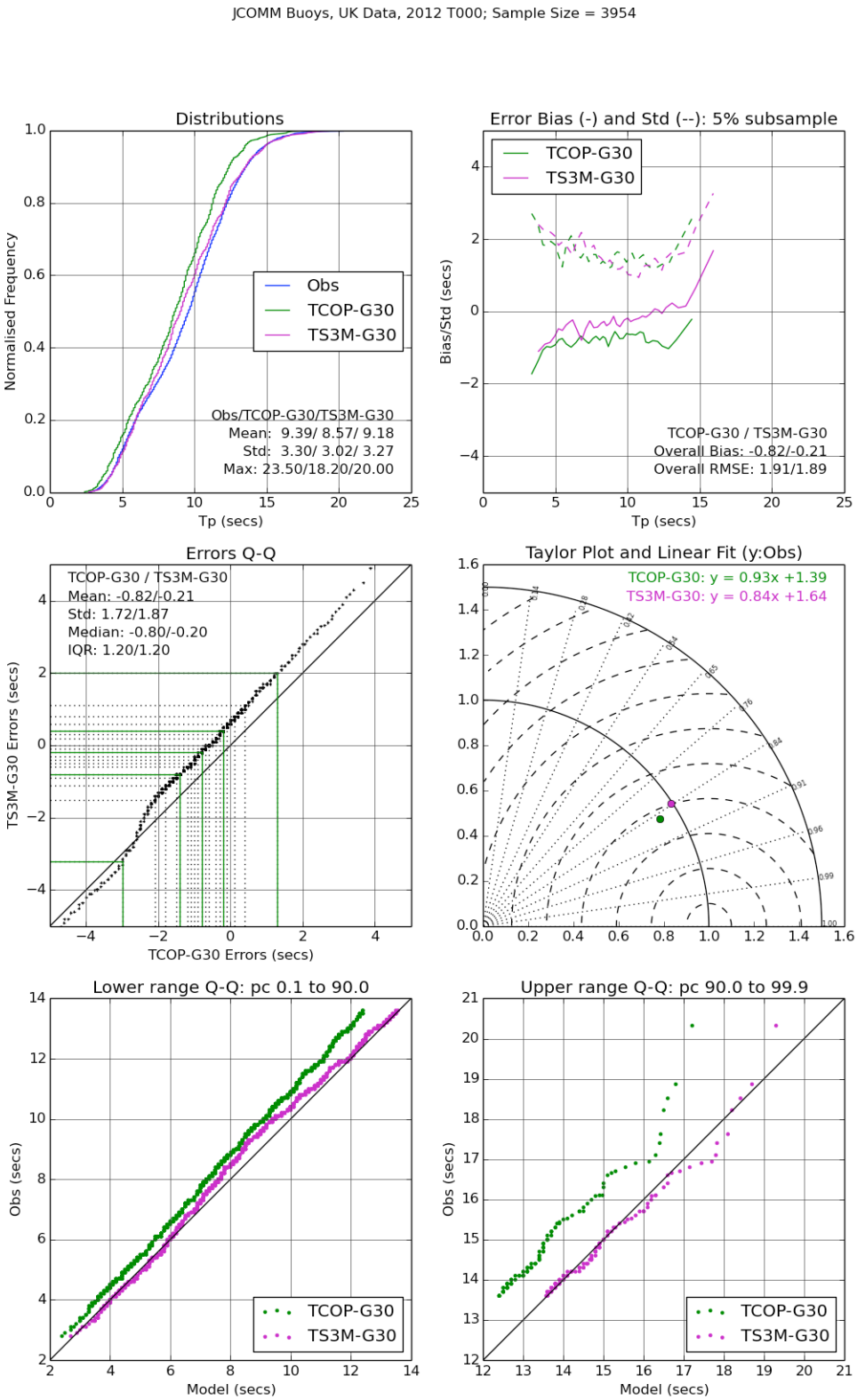

Figure 4.15. Peak period (Tp) verification against in-situ platforms for the TCOP and TS3M runs of the Global wave model. Statistics for UK region.

© Crown copyright 2011

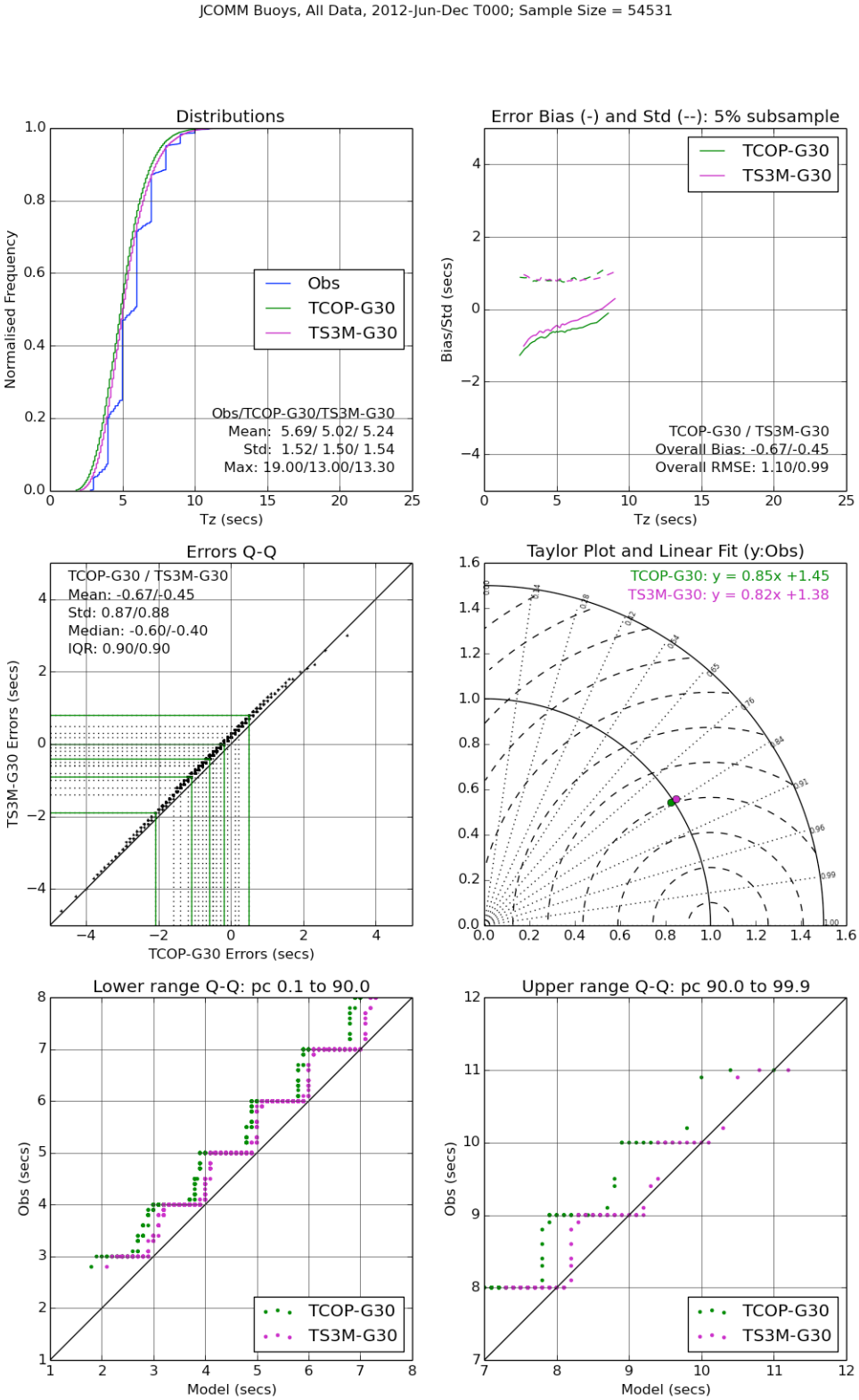

Figure 4.16. Mean zero-upcrossing period (Tz) verification against in-situ platforms for the TCOP and TS3M runs of the Global wave model. Statistics based on all available data.

© Crown copyright 2011

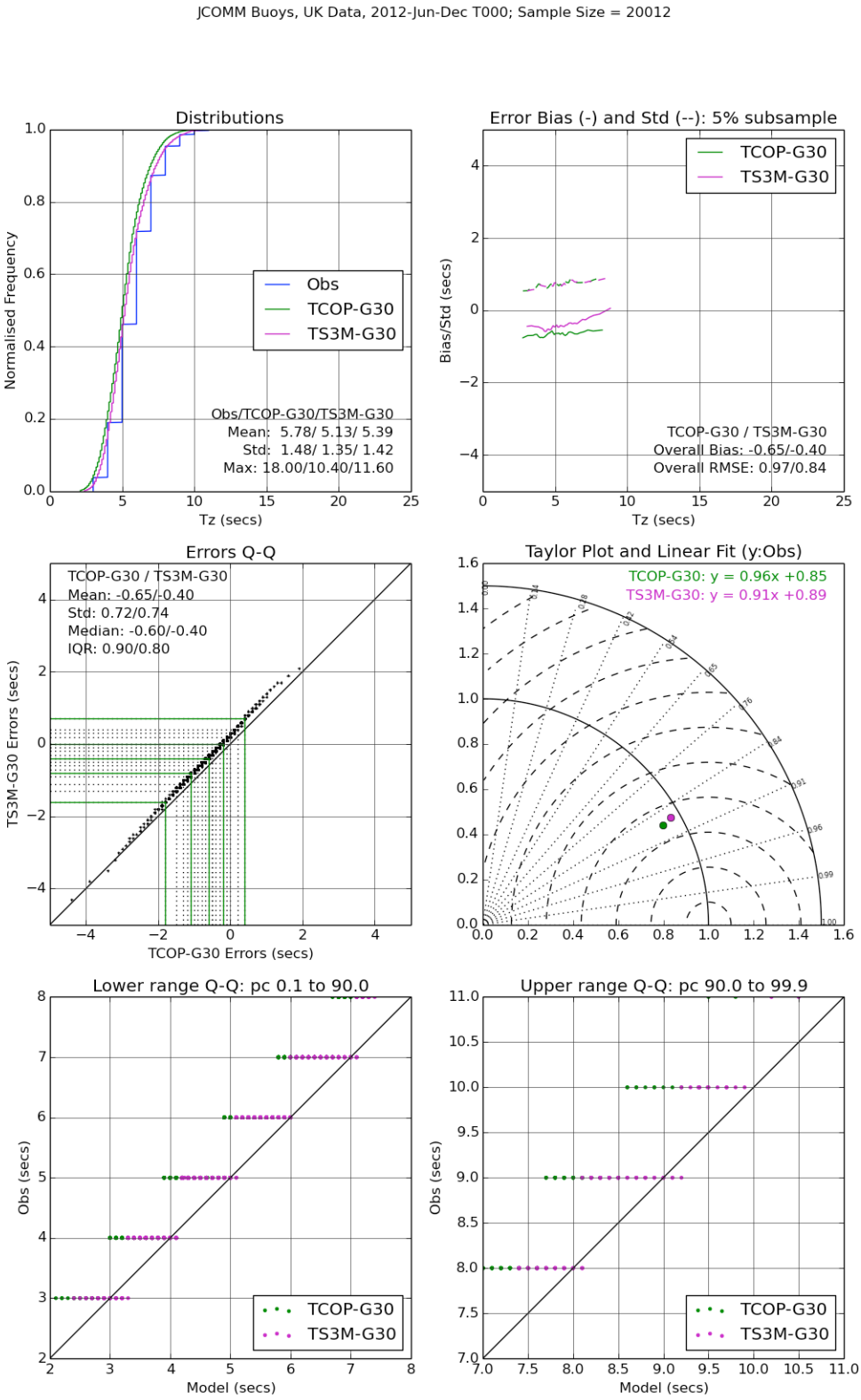

Figure 4.17. Mean zero-upcrossing period (Tz) verification against in-situ platforms for the TCOP and TS3M runs of the Global wave model. Statistics for UK region.

© Crown copyright 2011

4.3 In-situ observation verification in 'boundary condition' regions

In addition to wave forecasting in its own right, one of the primary roles of the global wave model is to provide high quality boundary conditions for the nested European and UK configurations. In-situ observations from close to these boundary regions (Figure 4.18) have been used to indicate the likely performance of TS3M versus TCOP as a boundary condition.

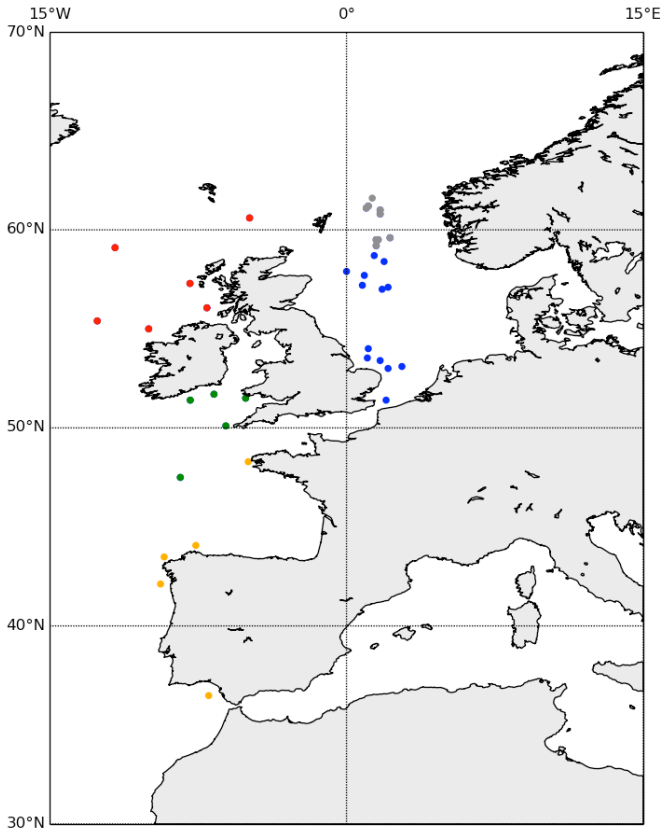

Figure 4.18. Locations of in-situ data platforms used for verification for UK and northwest European Atlantic margin. Subset regions discussed in subsequent figures are marked as Northern North Sea (grey), Northwest Approaches (red), Southwest Approaches (green), Iberian-Atlantic (orange).

© Crown copyright 2011

Figure 4.19 compares Hs verification in the Northern North Sea (east of Shetland). Overall, TS3M has a slightly reduced positive bias and RMSE, compared to TCOP (plot 2), but is also capable of reproducing the highest wave conditions (with a slight positive bias, plot 6) and has substantially reduced under-prediction errors (plot 3). TS3M is more positively biased than TCOP when predicting the largest storm waves (plot 2 and 3).

Figure 4.20 assess the Northwest Approaches to the UK (north of Ireland and west of Shetland). Here, TS3M has a slightly negative bias (relative to a significant positive bias for TCOP) and RMSE is reduced by approximately 6% (plot 2). TCOP is biased high for the higher wave conditions (plots 2 and 6), which are reproduced better by TS3M. A similar picture emerges for the comparison in the Southwest Approaches (Figure 4.21), although both models over-predict the observed wave heights above the 90th percentile (plot 2 and 6). In this region the RMSE for TS3M is reduced by 9% compared to that for TCOP.

Away from the UK, data from an Iberian-Atlantic region (including French and Spanish buoy data) are used to estimate performance for the European wave model's southwest boundary area (Figure 4.22). The verification in this region is consistent with that for the Southwest Approaches, although it is noted that, whilst TS3M replicates high wave conditions with a lower (positive) bias than TCOP (plot 6), error standard deviation for TS3M's high wave predictions is higher than for TCOP (plot 2).

© Crown copyright 2011

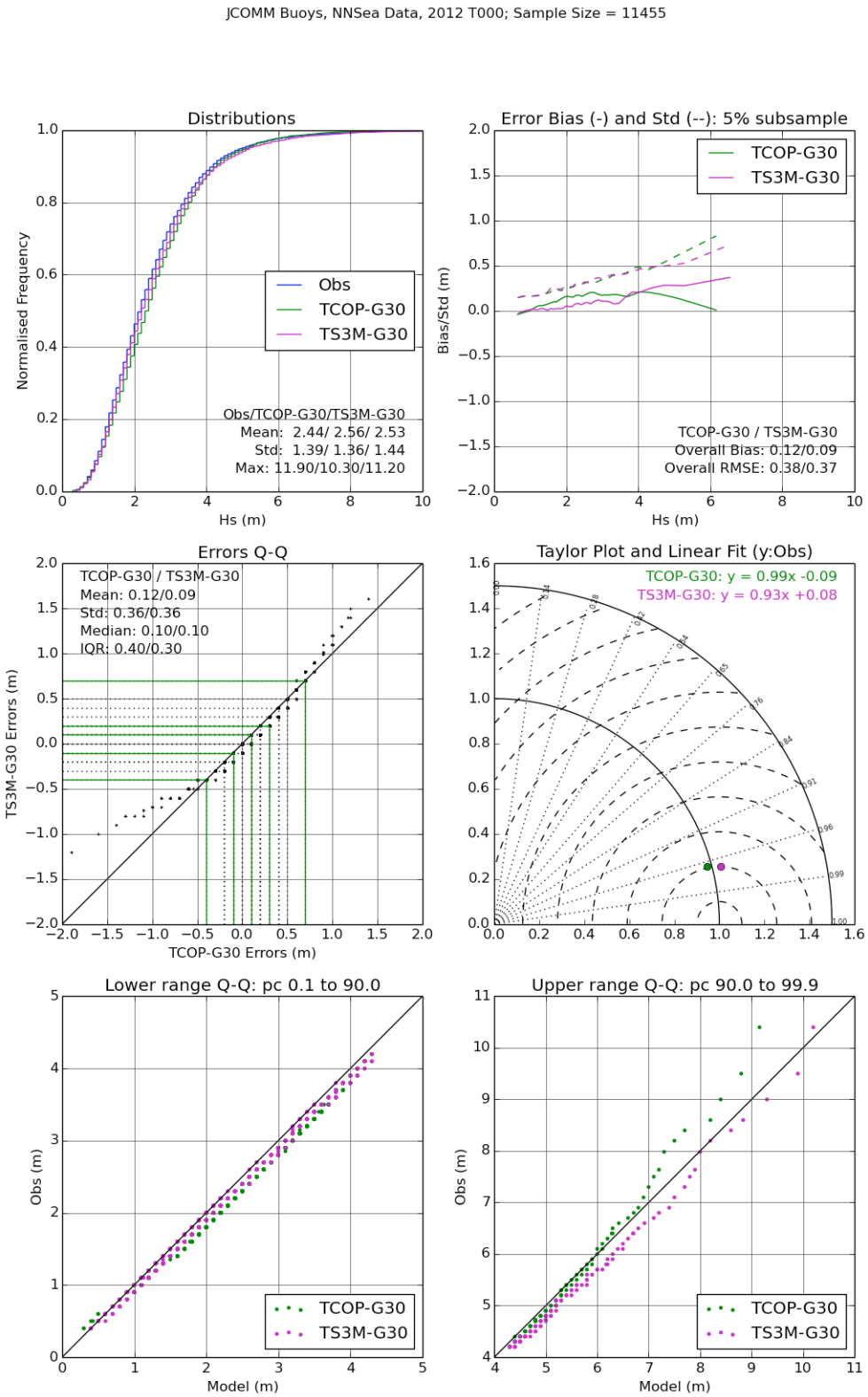

Figure 4.19. Significant wave height (Hs) verification against in-situ platforms for the TCOP and TS3M runs of the Global wave model. Statistics for northern North Sea region.

© Crown copyright 2011

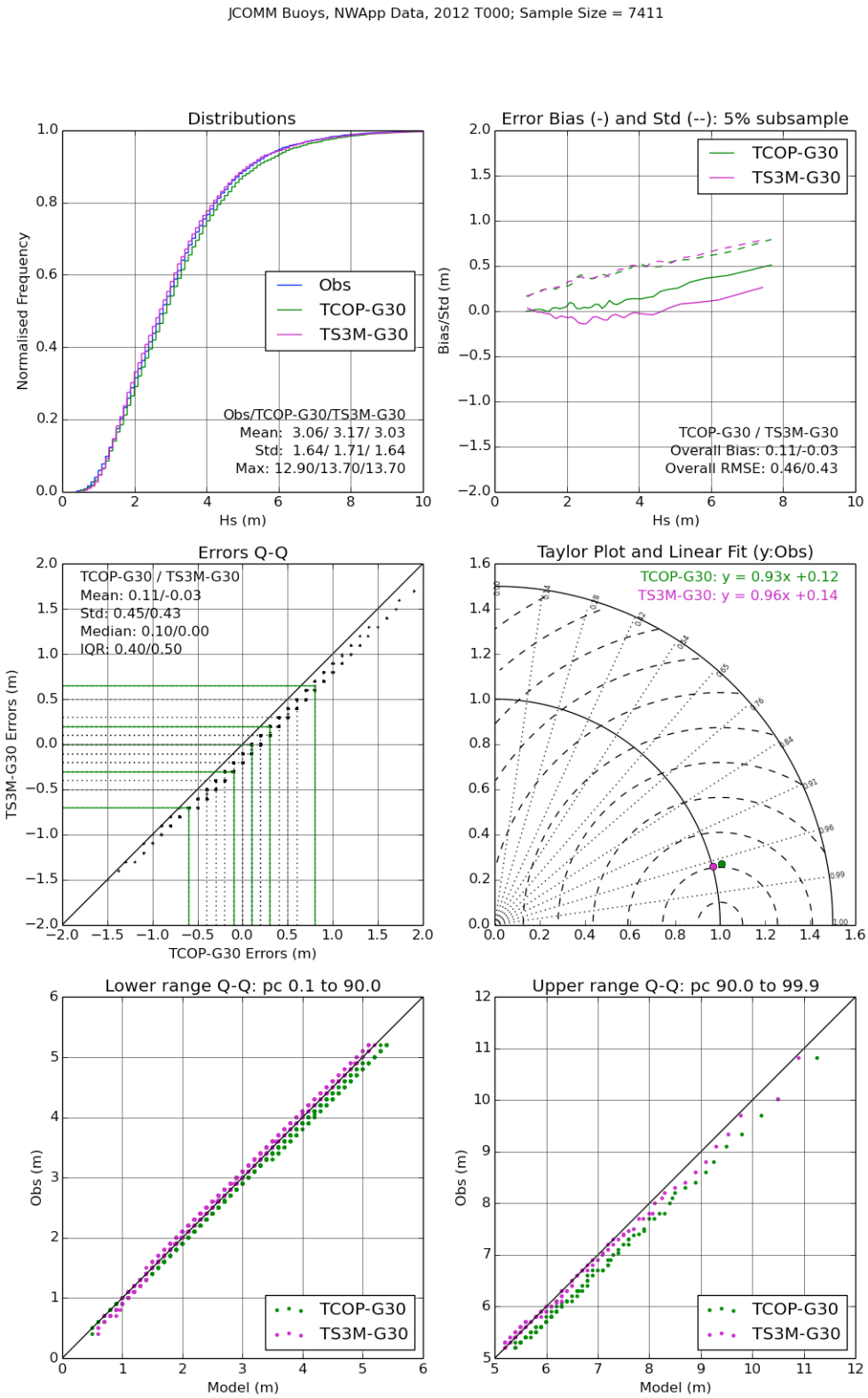

Figure 4.20. Significant wave height (Hs) verification against in-situ platforms for the TCOP and TS3M runs of the Global wave model. Statistics for Northwest Approaches region.

© Crown copyright 2011

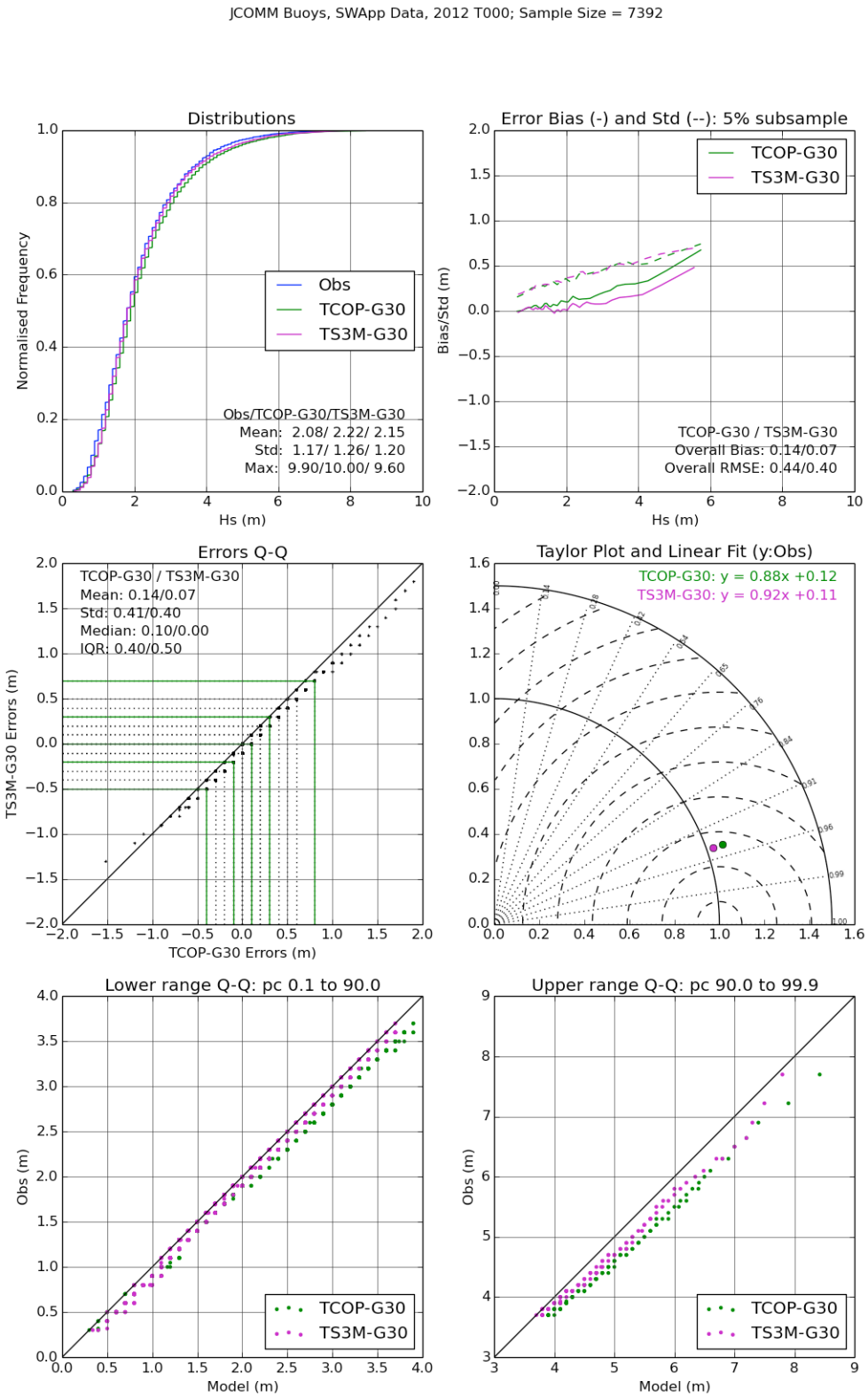

Figure 4.21. Significant wave height (Hs) verification against in-situ platforms for the TCOP and TS3M runs of the Global wave model. Statistics for Southwest Approaches region.

© Crown copyright 2011

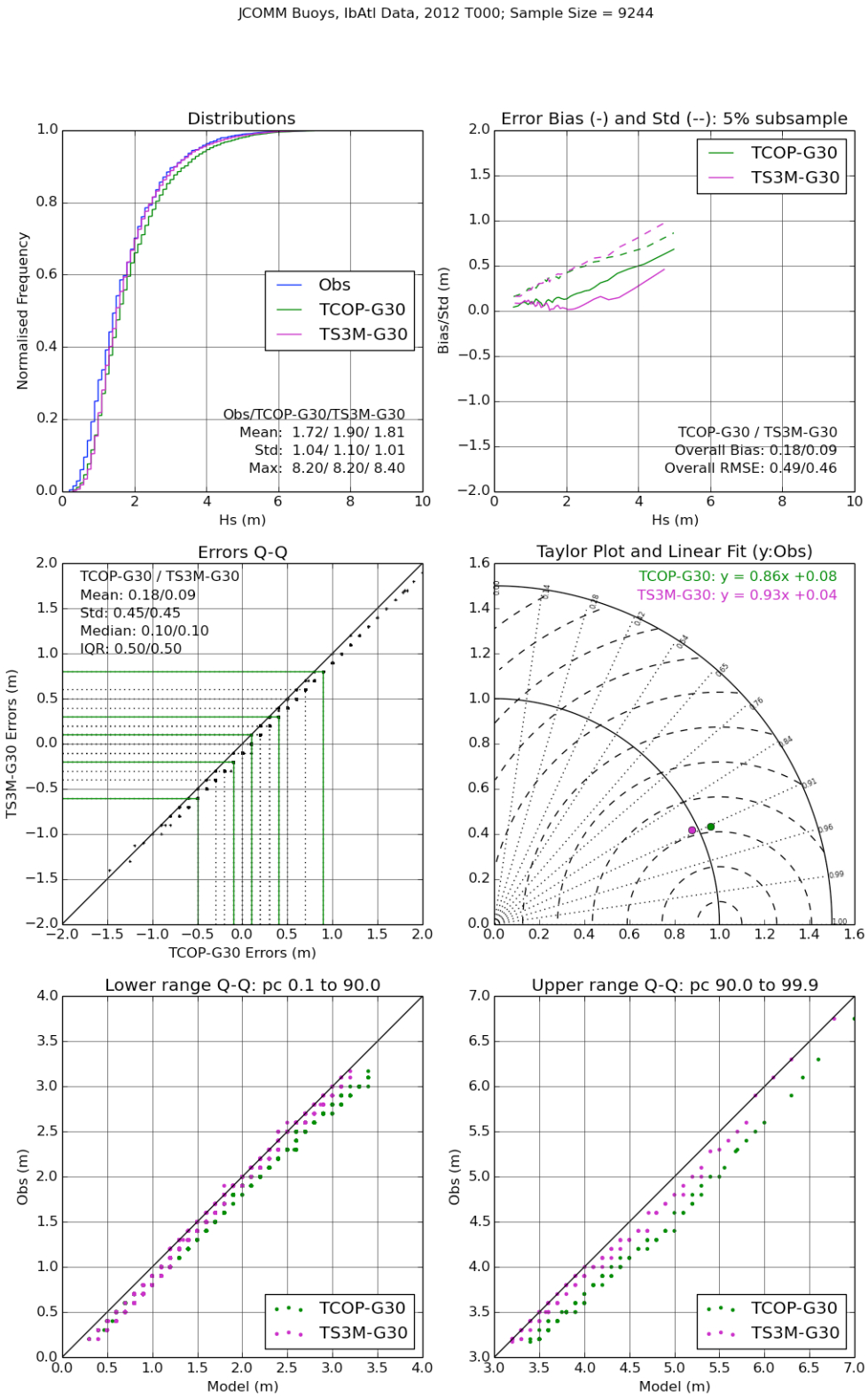

Figure 4.22. Significant wave height (Hs) verification against in-situ platforms for the TCOP and TS3M runs of the Global wave model. Statistics for Iberian-Atlantic region.

© Crown copyright 2011

5. Test3M impacts on regional wave models

Verification from the boundary regions suggests that running the global wave model using TS3M should lead to better lateral boundary conditions being supplied to the nested European and UK wave configurations. In the present operational set-up, both the UK and European domains use the EC12 physics scheme. If the same set-up were kept, predictions from the nested models should take on characteristics of EC12 away from the boundary region. The impact of changing the global physics scheme may therefore be reduced within any nested model verification.

In order to test this, 1 year (2012) runs were made for the European and UK configurations using both TCOP and TS3M boundary conditions. To assess the impact of a global model change for nested models in the UK, we concentrate on results from the UK configuration in this report. This is since the UK has the lowest distance between its boundaries and any verifying observation locations. Hs verification results are shown in Figure 5.1 for all buoys in the UK region (all sites in Figure 4.18). Differences between the two experiments were negligible. Picking out details, a small change in bias for high wave height predictions (plot 2) and a reduction in the extreme under-prediction error (plot 3) can be seen for the TS3M boundary condition model.

A geographic breakdown of bias and RMSE statistics, based on the observation groupings in Figure 4.18, is given in Table 2. The results suggest that, in terms of Hs prediction, there is little to choose between using the different boundary condition options. Changes in Tz verification were also generally neutral. Tp RMSEs were slightly negatively impacted in the TS3M run, although regionally there was evidence for an improvement in replication of the Tp climatology for more extreme events (over 90th percentile). Similar results were seen for the European configuration.

As a final test, versions of the UK and European configurations were also run using the TS3M boundary condition with the TS3M source term applied to the regional models. The results are shown in Figure 5.2 (for Hs for the whole UK region) and Table 2 (for a regional breakdown of bias and RMSE). In general, adopting TS3M for both global and regional models was found to be slightly detrimental to performance.

© Crown copyright 2011

Table 2. Regional breakdown of UK/European wave model Hs performance (bias/RMSE) for boundary condition (bc) and nested model physics tests.

	Boundary condition tests (config-bc type, nested models run EC12 physics)			**TS3M for bc and nested model physics (config)**	
Region	**UK-TCOP**	**UK-TS3M**	**EU-TS3M**	**UK**	**Global**
North North Sea	0.12 / 0.36	0.14 / 0.37	0.07 / 0.35	0.17 / 0.39	0.09 / 0.37
Central North Sea	-0.01 / 0.30	0.04 / 0.30	0.01 / 0.31	0.07 / 0.32	0.09 / 0.35
South North Sea	0.01 / 0.22	0.02 / 0.22	0.02 / 0.23	0.04 / 0.23	0.05 / 0.25
Irish Sea	-0.12 / 0.23	-0.12 / 0.23	-0.11 / 0.22	-0.10 / 0.22	-0.07 / 0.23
NW Approaches	-0.05 / 0.42	-0.07 / 0.41	-0.10 / 0.43	-0.07 / 0.42	-0.03 / 0.43
SW Approaches	0.01 / 0.33	0.00 / 0.33	0.00 / 0.33	0.01 / 0.35	0.07 / 0.40
Iberian-Atlantic	N/A	N/A	0.06 / 0.39	N/A	0.09 / 0.46
Mediterranean	N/A	N/A	-0.12 / 0.30	N/A	-0.02 / 0.38

© Crown copyright 2011

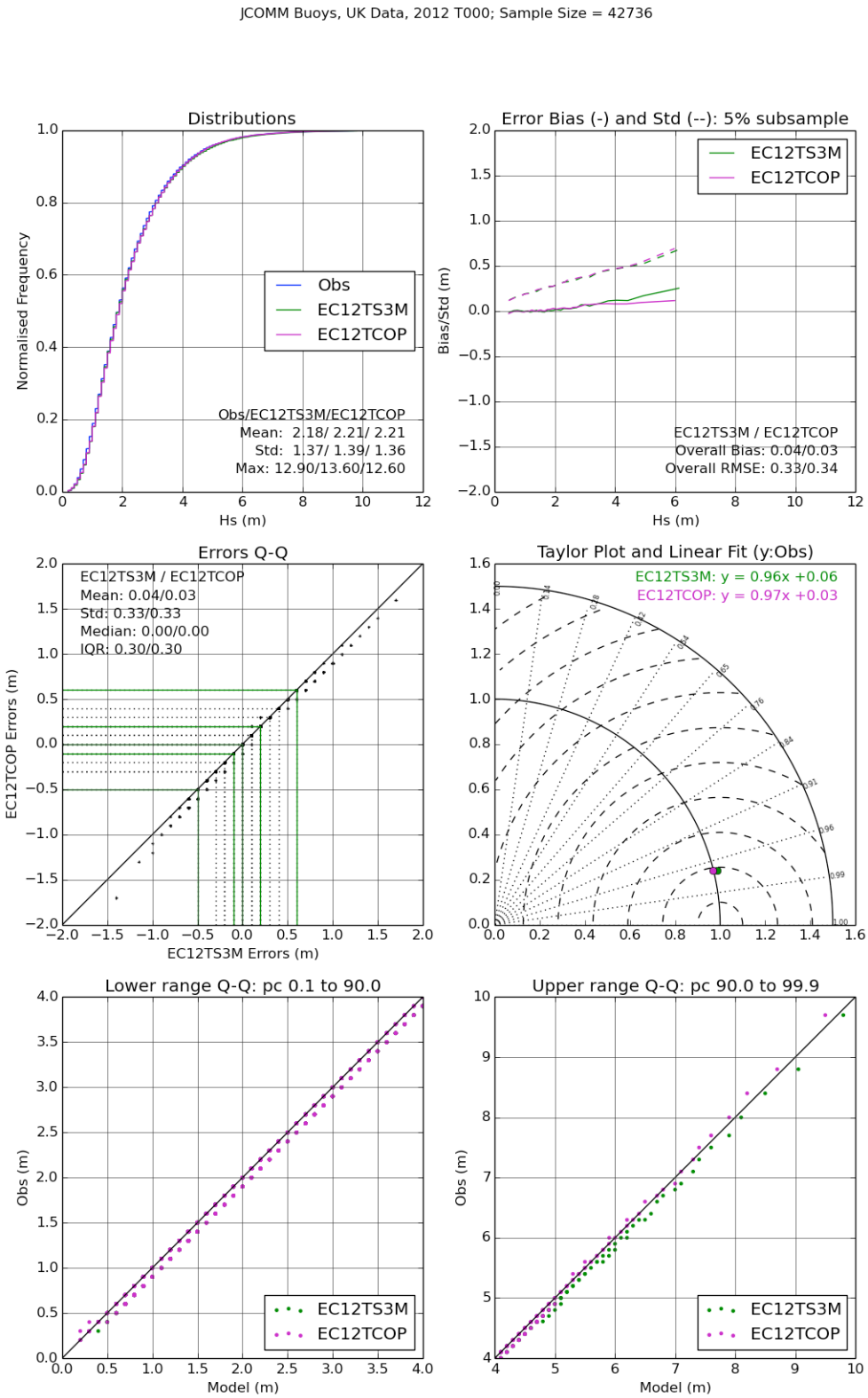

Figure 5.1. Significant wave height (Hs) verification against in-situ platforms for an EC12 run of the UK wave model using the TCOP and TS3M runs of the Global wave model as boundary conditions. Statistics for UK region.

© Crown copyright 2011

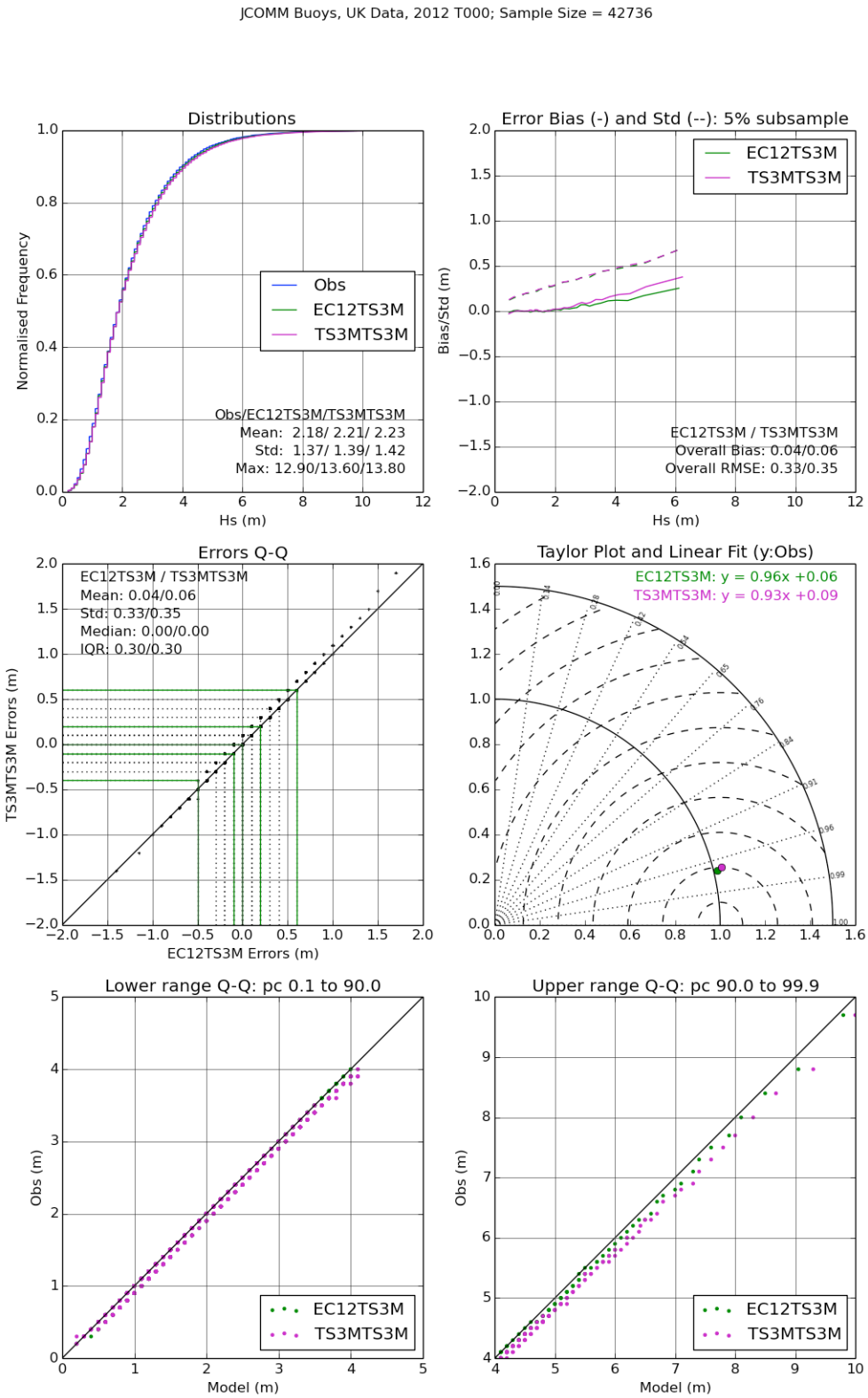

Figure 5.2. Significant wave height (Hs) verification against in-situ platforms for EC12 and TS3M runs of the UK wave model using the TS3M run of the Global wave model as boundary conditions. Statistics for UK region.

© Crown copyright 2011

6. Spatial impacts of transition from TCOP to TS3M

To assess the relative change in model behaviour as a result of a transition of the global model from TCOP to TS3M, this section examines relative changes in the TS3M-TCOP the model climatology. This exercise can be performed for any region globally but, for the purposes of this report, the concentration here is on the North Atlantic (Metarea 1) region of the global wave model and the UK regional model.

Figures 6.1 and 6.2 show changes in mean and variance of Hs and Tp for the global model in the North Atlantic. The anomalies use TS3M minus TCOP as a convention, i.e. a negative anomaly occurs when the TCOP parameter is higher. On average, Hs predictions for the North Atlantic are expected to be slightly lower than in the present model, with the most major changes seen in the western approaches to the UK and France and the southwest quadrant of the North Atlantic. Average wave height predictions will be raised along the eastern seaboard of North America and Greenland. Variability in significant wave height is diminished in the eastern North Atlantic, where seas are likely to be more mature, and increased in young wind-sea generation regions in the northwest of the ocean basin. However, the variability changes are small (approximately 5-10%) relative to background variance in Hs. Peak period values will be generally increased in the TS3M model, by approximately 0.5-1 seconds on average. Variability of Tp is also increased, mainly in the southeast of the domain.

Figures 6.3 and 6.4 show the same Hs and Tp parameters for the UK regional model. In these cases the UK model uses the EC12 scheme, so any changes result from the revised global boundary condition. Toward the western boundary, the annual mean Hs values will be lower, with a small reduction being maintained further into the model domain in the southwest approaches. The change toward the northern boundary of the model should be small, but the overall effect of applying the TS3M boundary condition will be a slight positive shift in wave heights west of Shetland and in the northern and central parts of the North Sea. Overall the variability in model wave heights will be increased slightly, with the strongest effect in the northwest approaches. Peak periods will be generally increased, both in terms of the mean and variability, although the effect tends to be diminished away from the boundary region. A similar analysis of Tz showed very little change versus the background levels.

© Crown copyright 2011

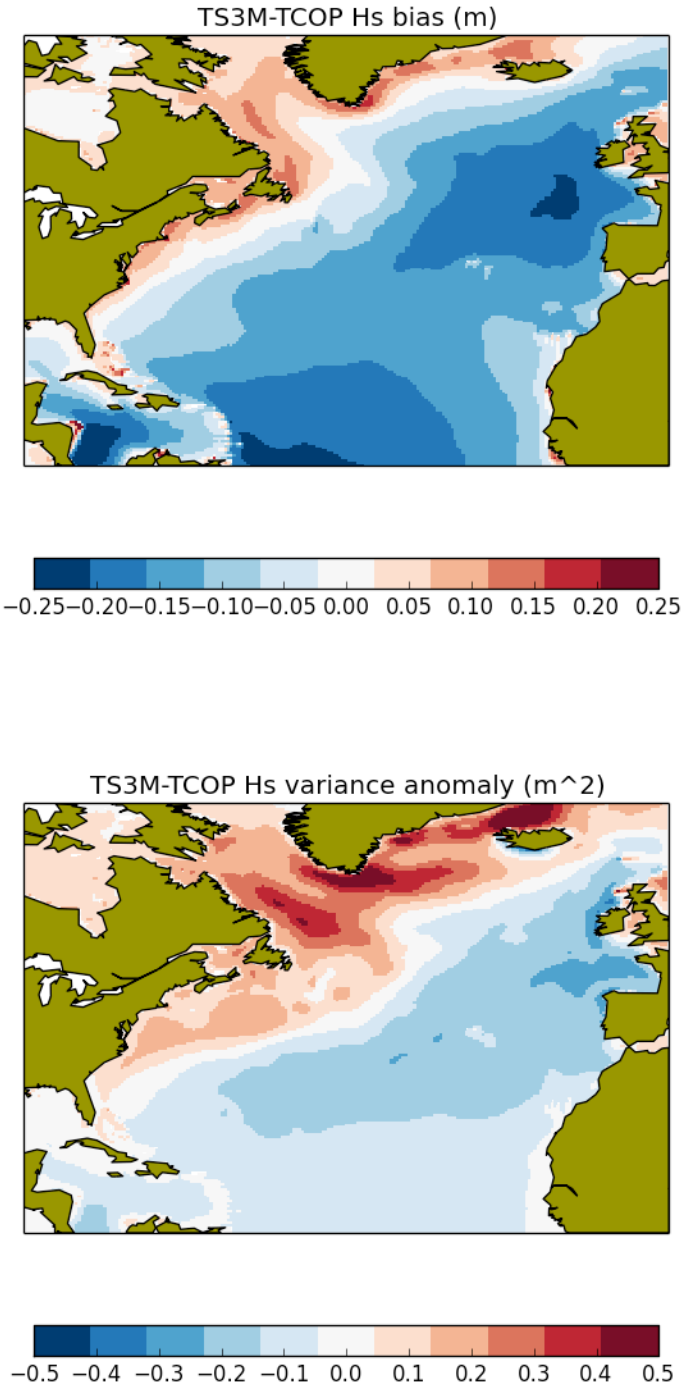

Figure 6.1. Difference in 2012 North Atlantic Hs data for global wave model run using TS3M versus a run with TCOP. Top panel shows mean Hs bias; bottom panel shows change in Hs variance (TS3M-TCOP).

© Crown copyright 2011

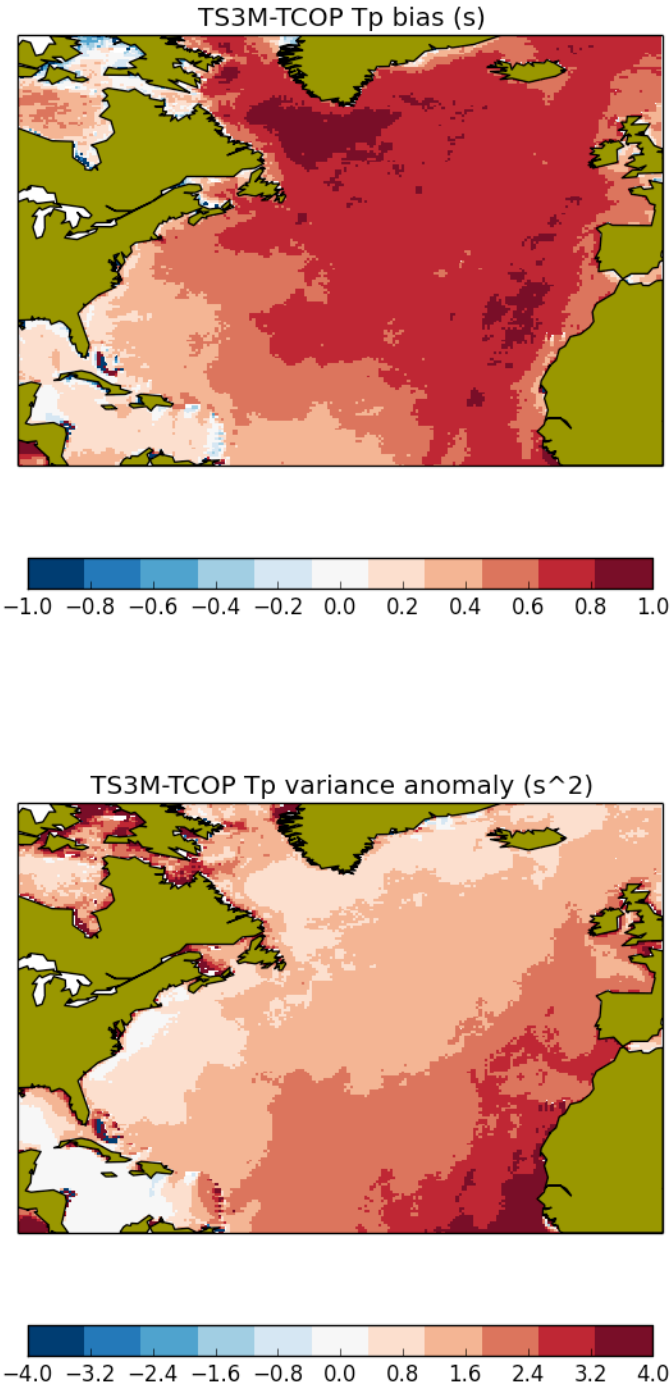

Figure 6.2. Difference in 2012 North Atlantic Tp data for global wave model run using TS3M versus a run with TCOP. Top panel shows mean Tp bias; bottom panel shows change in Tp variance (TS3M-TCOP).

© Crown copyright 2011

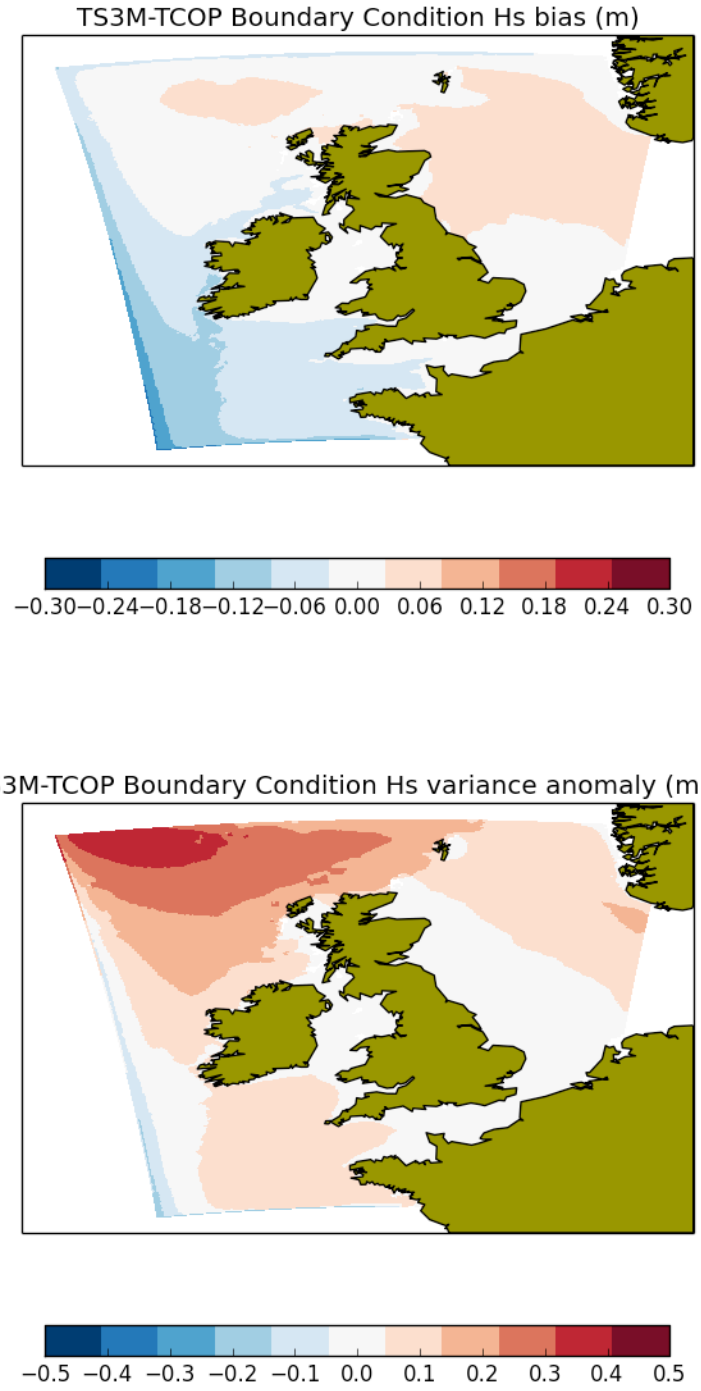

Figure 6.3. Difference in 2012 Hs data for UK wave model run (based on EC12 physics) using TS3M boundary conditions versus a run with the TCOP boundary condition. Top panel shows mean Hs bias; bottom panel shows change in Hs variance (TS3M-TCOP).

© Crown copyright 2011

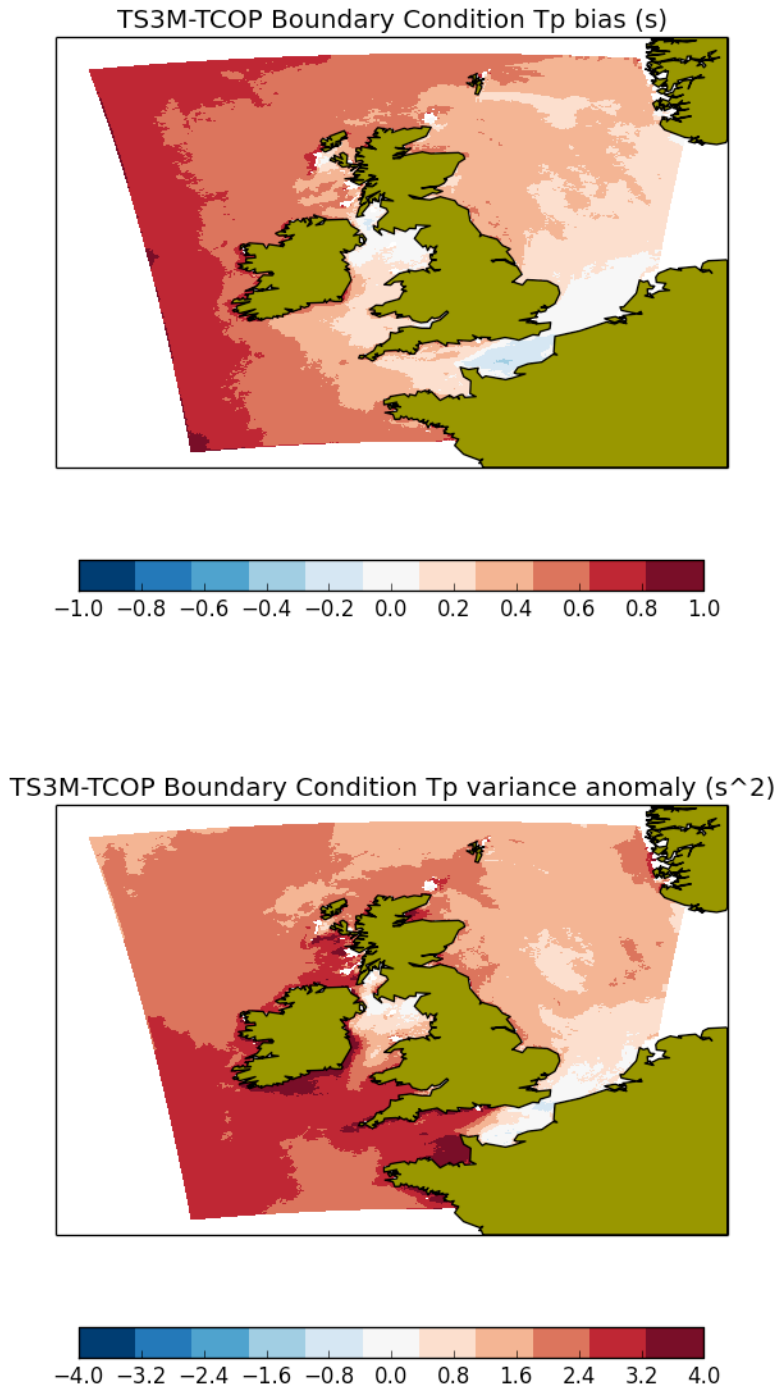

Figure 6.4. Difference in 2012 Tp data for UK wave model run (based on EC12 physics) using TS3M boundary conditions versus a run with the TCOP boundary condition. Top panel shows mean Tp bias; bottom panel shows change in Tp variance (TS3M-TCOP).

© Crown copyright 2011

7. Conclusions and discussion

The principal purpose of this work has been to characterise behaviours of a number of different flavours of wave model source term physics, available in WAVEWATCH III vn3.14, with a view to selecting a package that can be adopted in the Met Office global wave model. All the physics tested have strong points and weaknesses in terms of their process representation, but the study was able to identify a successor package to the Tolman and Chalikov (1996) source terms (which have been used in the Met Office global wave model since November 2008). The new scheme follows the wave growth and dissipation parameterisations of WAM Cycle-4, but also includes terms following Ardhuin et al. (2010) in order to account for dissipation in swell dominated conditions. The source terms will continue to use the DIA scheme to represent nonlinear four-wave interactions. Details of wave model settings for the scheme, TS3M, are given in Table 1 of this document.

Compared to the present operational scheme, verification has suggested that TS3M will lead to an approximate 5% improvement in significant wave height RMSE and a 10% improvement in mean zero-upcrossing period RMSE. The majority of these improvements will be expected to be obtained in mid-high latitude storm tracks, in association with development of wind-sea during developing storms over short to moderate fetches. These improvements are offset by a negative significant wave height and positive peak period bias in regions of the global ocean that are dominated by mature wind-seas and swell. Overall impacts of the change to the global physics on regional wave models run at the Met Office are expected to be negligible. The verification suggests however that the spectral boundary conditions fed to the regional models under storm conditions may be increased relative to the present system. The verification has also confirmed that no performance gain can be made by implementing TS3M as a ‘one size fits all’ physics package applied to regional models for UK and Europe as well as in the global model.

It is anticipated that the TS3M scheme will be introduced to the Met Office operational global wave model in early 2015, following Parallel Suite 35.

7.1. Discussion

This study has focused on assessing relative behaviours of different source terms and tuning parameterisations in order to obtain an optimal configuration that can be used in an operational wave model. The study verification results and conclusions were drawn

© Crown copyright 2011

from results of a year-long analysis of wave data. Observations were assumed to be representative of true sea-state (an alternative interpretation is that the verification tests consistency with the model and observed conditions). The errors that were analysed will be a product of both errors in the wave model and errors in the forcing winds. As with most model studies, the possibility that the wave model component has been somewhat tuned to compensate for wind errors cannot be ruled out.

In deciding what 'optimal' looked like, a limited consideration of the theoretical background to each source term scheme was made. The only conclusion that can be drawn from this study is that, although the schemes can be shown to have different strengths and weaknesses, none of the source term packages tested appeared to be universally better or worse than the other options (even if some might adopt theoretically higher ground). This is an evolving branch of wave modelling, particularly in terms of the development of dissipation parameterisations (e.g. following Ardhuin et al., 2010; Filipot and Ardhuin, 2012). It should also be noted that the use of WAVEWATCH vn3.14 (as the present flavour of operational model code) limited the study. For example, we have not tested against some of the latest modifications to the 'Ardhuin et al.' group of physics schemes released publicly in WAVEWATCH III vn4.18.

The spectral development tests in Section 2 show the strong influence that the DIA scheme has on the wave spectrum. It may be that common use of the DIA has a moderating effect on the differences between other source term parameterisations. It can be argued that a truer test of the source terms would be to run these simulations with a more 'exact' solution to the nonlinear wave interaction equations. However, the aim in this test was to analyse the source terms within the context of a practicable operational forecast model.

Whilst not highlighted in this report, part of the final choice of source term was driven by examining seasonal performance of the model. Seasonality can have a strong effect on the verification, for example where neutral biases in the annual data mask strong, compensating, positive and negative biases at different times of year. For example, seasonal variability in Hs bias and RMSE was particularly noticeable for regions affected by monsoon weather systems (such as the Arabian Sea). The existence of such features highlight the fact that the choices made in selecting a global model configuration are likely to be a compromise, and that regional details of performance should be monitored and documented following model implementation.

The verification has concentrated on significant wave height, peak period and zero-upcrossing period as indicators of model performance. In future, the process of model

© Crown copyright 2011

validation could be improved by adding more detailed verification of wave spectra against available in-situ spectral observations. The model tuning process also has the potential to be improved if a better understanding of the long term mix of sea conditions (wind-sea, swell) specific to given regions of the global oceans can be obtained. This might be achieved through making a more detailed study of long term wave age time-series and distances of travel for swell systems reaching different locations (e.g. Perez et al, 2014).

© Crown copyright 2011

8. References

Ardhuin, F., E. Rogers, A.V. Babanin, J.-F. Filipot, R. Magne, A. Roland, A. Van der Westhuysen, P. Queffeulou, J.-M. Lefevre, L. Aouf and F. Collard, 2010: Semi-empirical dissipation source functions for wind-wave models. Part I: definition, calibration and validation. J. Phys. Oceanogr., 40 (9), 1917–1941.

Bidlot, J.-R., 2012: Present status of wave forecasting at E.C.W.M.F. In Proc. ECMWF Workshop on Ocean Waves, Reading, 2012, p1-15.

Bidlot J.-R., D. J. Holmes, P.A. Wittmann, R. Lalbeharry, H. S. Chen, 2002: Intercomparison of the performance of operational ocean wave forecasting systems with buoy data. Wea. Forecasting, 17, 287-310.

Bidlot, J.-R., J.-G. Li, P. Wittmann, M. Faucher, H. Chen, J.-M, Lefevre,T. Bruns, D. Greenslade, F. Ardhuin, N. Kohno, S. Park and M. Gomez, 2007: Inter-Comparison of Operational Wave Forecasting Systems. In Proc. 10th International Workshop on Wave Hindcasting and Forecasting and Coastal Hazard Symposium,North Shore, Oahu, Hawaii, November 11-16, 2007.

Breugem, W.A. and L.H. Holthuijsen, 2006: Generalised wave growth from Lake George. J. Waterway, Port, Coastal and Ocean Engineering, ASCE.

Hasselmann, S., K. Hasselmann, J.H. Allender, and T.P. Barnett, 1985: Computations and parameterisations of the nonlinear energy transfer in a gravity wave spectrum. Part 2: Parameterisations of the nonlinear energy transfer for application in wave models. J. Phys. Oceanogr., 15, 1378-1391.

Komen, G., L. Cavaleri, M. Donelan, K. Hasselmann, H. Hasselmann and P.A.E.M. Janssen, 1994: Dynamics and Modelling of Ocean Waves, Cambridge Univ. Press, 532pp.

Perez, J., F. Mendez, M. Menendez, and I.J. Losada, 2014: ESTELA: a method for evaluating the source and travel time of the wave energy reaching a local area. Ocean Dynamics, DOI: 10.1007/s10236-014-0740-7.

Tolman, H.L., 2009: User manual and system documentation of WAVEWATCH III™ version 3.14. NOAA / NWS / NCEP / MMAB Technical Note 276, 194 pp + Appendices.

© Crown copyright 2011

Tolman, H. L., and D. Chalikov, 1996: Source terms in a third-generation wind-wave model. J. Phys. Oceanogr, 26, 2497-2518.

© Crown copyright 2011

Met Office
FitzRoy Road, Exeter
Devon EX1 3PB
United Kingdom

Tel (UK): 0870 900 0100 (Int) : +44 1392 885680
Fax (UK): 0870 900 5050 (Int) :+44 1392 885681
enquiries@metoffice.gov.uk
www.metoffice.gov.uk